21108

NATIONAL LIBRARY
OTTAWA

BIBLIOTHÈQUE NATIONALE
OTTAWA

NAME OF AUTHOR.....HARBHAJAN SINGH.....

TITLE OF THESIS....Some Studies of Capsule
.....pipelining....I. Pipeline Capacity Correlations
.....II A theoretical model for laminar flow.

UNIVERSITY....of Alberta.....

DEGREE FOR WHICH THESIS WAS PRESENTED.....Ph.D.....

YEAR THIS DEGREE GRANTED.....1974.....

Permission is hereby granted to THE NATIONAL LIBRARY OF CANADA to microfilm this thesis and to lend or sell copies of the film.

The author reserves other publication rights, and neither the thesis nor extensive extracts from it may be printed or otherwise reproduced without the author's written permission.

(Signed).....Harbhajan Singh

PERMANENT ADDRESS:

#5 9515 - 104 st.
.....Edmonton.....
.....

DATED.May...6,.....19 74

NL-91 (10-68)

THE UNIVERSITY OF ALBERTA

SOME STUDIES ON CAPSULE PIPELINING:
I. EMPIRICAL CAPACITY CORRELATIONS;
II. A THEORETICAL MODEL FOR LAMINAR FLOW

by

© HARBHAJAN SINGH

A THESIS

SUBMITTED TO THE FACULTY OF GRADUATE STUDIES AND RESEARCH

IN PARTIAL FULFILMENT OF THE REQUIREMENTS FOR THE DEGREE

OF DOCTOR OF PHILOSOPHY

IN

CHEMICAL ENGINEERING

DEPARTMENT OF CHEMICAL ENGINEERING

EDMONTON, ALBERTA

(SPRING, 1974)

THE UNIVERSITY OF ALBERTA

FACULTY OF GRADUATE STUDIES AND RESEARCH

The undersigned certify that they have read, and recommend to the Faculty of Graduate Studies and Research, for acceptance, a thesis entitled SOME STUDIES ON CAPSULE PIPELINING: I. EMPIRICAL CAPACITY CORRELATIONS; II. A THEORETICAL MODEL FOR LAMINAR FLOW submitted by Harbhajan Singh in partial fulfilment of the requirements for the degree of Doctor of Philosophy in Chemical Engineering.

Donald Brown
.....
Supervisor

F.A. Seyer
.....

.....

R. Haardgrave
.....

.....

Norman Epstein
.....
External Examiner

Date April 26, 1974.

ABSTRACT

The concept of transporting solids in the form of capsules in pipelines evolved at the Research Council of Alberta during the fifties. Since then extensive experimental data have been generated but as yet no satisfactory correlations are available covering all the physical variables.

The data available from the Research Council of Alberta have been analysed using Bayesian statistical methods. Capacity correlations have been obtained for pipe sizes ranging from 1/2" to 10" in diameter. Little success, however, has been obtained in modeling the pressure drop in the system.

The second approach to the problem is fluid mechanics modeling. A preliminary physical model envisaging the capsule flow as consisting of a series of infinitesimal parallel slipper bearings is given here. Using a set of simplifying assumptions including one which neglects secondary flows, capacity and pressure drop correlations have been developed for laminar flow. As expected from the assumptions made, the model predictions for both the bulk velocity and pressure gradient for a given capsule velocity are lower than the observed values. However, addition of only one empirical parameter in each correlation for a given pipeline system gives reasonable agreement with the observed values. It is expected that substantial improvements in predictions would result if secondary flows can be incorporated in the model.

ACKNOWLEDGEMENT

The author wishes to express his appreciation of the criticism and guidance provided by Dr. D. Ouon who supervised this work. I am thankful to Dr. F. A. Seyer for his advice and guidance in the theoretical work, Dr. D. J. Wilson for suggesting the slipper bearing approach and Dr. C. A. Shook for very helpful comments and criticism on the pressure flow in Chapter 3. The author also wishes to express his appreciation for the help and cooperation received from Messrs. F. Jensen, H. S. Ellis and J. Kruyer of the Research Council of Alberta, Edmonton, Alberta.

Thanks are due to Mrs. Lynda Masse and Mrs. Lola Logan for patience in this difficult typing and due thanks to Mr. K. K. Chawla for providing the drafting services.

This work was carried out under a grant from the Research Council of Alberta through their contract from Transport Development Agency of the Ministry of Transport.

TABLE OF CONTENTS

1. INTRODUCTION 1

1.1 Capsule Flow 1

1.1.1 Historical 1

1.1.2 Empirical Work 2

1.1.3 Theoretical Development 5

1.2 Experimental Set-up 6

1.3 Model Discrimination and Model Building 12

1.3.1 Mathematical Modeling 12

1.3.2 Model Discrimination and Estimation 13

1.3.3 Tests of Model Adequacy 16

1.3.4 Model Improvement and Model Generation 17

2. EMPIRICAL CORRELATIONS 20

2.1 Scope 20

2.2 Physical Variables 20

2.3 Experimental Data 22

2.4 Capacity Correlations 24

2.5 Towards a General Correlation 37

2.5.1 Dimensional Analysis 37

2.5.2 Incorporating Empirical Observations 39

2.5.3 Flow Regimes 41

2.6 Pressure Gradients 45

3. A THEORETICAL MODEL FOR THE LAMINAR PIPE FLOW OF CAPSULES 51

3.1 Scope 51

3.2 A Preliminary Physical Model 52

TABLE OF CONTENTS (Continued)

3.3 Couette Flow 54

3.3.1 Plane Slipper Bearing 54

3.3.2 Capsule Couette Flow Model 63

3.4 Pressure Flow 68

3.5 Total Flow 73

3.6 Physical Contact of Surfaces 78

3.7 Threshold Velocity 81

3.8 Model Validation 81

4. CONCLUSIONS

4.1 Summary 89

4.2 Further Work 90

BIBLIOGRAPHY 95

APPENDIX A 99

APPENDIX B 100

APPENDIX C 102

APPENDIX D 104

APPENDIX E 107

APPENDIX F 109

APPENDIX G 111

1. INTRODUCTION

1.1 Capsule Flow

1.1.1 Historical

The development of solids transportation through pipelines has not played a significant role in our overall technological growth. The concept was suggested in California as early as 1850. The first practical application, however, did not materialize until 1914 when an 8-inch cast iron pipeline 1750 feet long, was built to transport coal slurries from the London docks to power stations. By 1959, some 20 pipelines were carrying 30 million long tons annually of mixtures of phosphate rock, sand and clay. During the fifties and sixties, pipelines were installed for transporting varieties of solids including ore concentrates, limestone, phosphate and coal (1).

New developments in slurry pipelining depend largely on solving a host of technical problems. Some of the problems arise in processing the solids before pumping, keeping the solids in suspension during transportation and separating the solids from the carrying fluid and drying. Abrasive action of solids in the pipeline may demand special material or design for the pipeline.

A novel departure from the established solids pipeline methods was suggested by the findings of Charles, Govier and Hodgson (2) on the flow of oil in the presence of water. If water and oil of the same density flow through a pipeline, stable spherical or cylindrical slugs of oil in water or water in oil can be formed. Furthermore, these bubbles could be equal density solids and subsequent experimental tests

indeed proved that this mode of solids transportation was feasible. The idea was later extended to solids capsules heavier than that of the carrying liquid.

1.1.2 Empirical Work

Experimental work has been going on in the area of capsule flow at the Research Council of Alberta since 1958. The aim of the program is to obtain sufficient understanding of the capsule flow system for a rational assessment and design of a commercial installation. In an attempt to obtain the dependence of capsule velocity and pressure gradient on the capsule, the carrying liquid and the pipe characteristics, several empirical studies have been reported (3, 4, 5, 6, 7, 8, 9). The bulk of the work has been done at the Research Council of Alberta, Edmonton, Alberta. Some quantitative relationships have been obtained for specific conditions. The main results for cylindrical capsules may be summarized as follows.

The capsule travels at a slight angle to the axis of the pipe, generally with a nose-up position. The clearance at the capsule bottom is extremely small, being barely visible, even for capsules of density nearly equal to that of the carrying liquid (say within 2%). Over a rather wide range of operating conditions, capsule velocity is found to be roughly equal to (within $\pm$ 20%) the bulk velocity of the liquid. The capsule length/diameter ratio and end shapes have little effect on the capsule velocity and pressure gradients for capsule length/diameter ratios greater than 6.

The capsule velocity is also found to vary linearly with liquid bulk velocity except at very low velocities, for a given system of

capsule, carrying liquid and pipeline. Pressure gradients, however, follow no simple relationship with the liquid bulk velocity. Velocity measurements have relatively small variance and are generally reproducible. While pressure drop measurements are reproducible on the run to run basis it was found they were not reproducible on certain pipelines after extensive experimentation suggesting some change in the experimental conditions. Variances of the capsule velocity measurements and that of the pressure drop measurements vary inversely with the viscosity of the carrying liquid, with the capsule to pipe diameter ratio and with the difference between the capsule and liquid densities. These inferences are drawn from the plots of the raw data obtained from the Research Council of Alberta.

The pressure drop is lowest and the velocity ratio (defined as capsule velocity divided by liquid bulk velocity) is highest when the capsule density is equal to that of the liquid. In particular, pressure drop is very sensitive to capsule density, increasing rapidly with increase in capsule density. No simple relationship can be established between the pressure drop and capsule/pipe diameter ratio, although, generally the velocity ratio increases with increasing diameter ratio. The data are not sufficient to establish the effect of the liquid viscosity on the pressure drops and the velocity ratios. However, there are indications that for a given capsule/pipe system, increasing the liquid viscosity from a low initial value, decreases the pressure drop while velocity ratio increases up to a certain point. Further increases in viscosity cause an increase in the pressure drop and a decrease in the velocity ratios.

Velocity ratios and pressure gradients are not significantly different for a train of capsules carrying many capsules from those for a single capsule. The line fill and spacing among the capsules also has only minor effects on the velocity ratios and pressure drops.

Another interesting empirical observation recently made by Ellis and Kruyer (10) is that pressure gradients are substantially (75-80%) reduced, with attendant increase of the capsule/liquid velocity ratio, by fitting the front half of the capsule with a collar. Sledge-type runners to lift the capsule off the bottom of the pipe are also successful in reducing the pressure drop but are not quite as effective as the collars.

Some attention has been given to the type of materials that can be transported and the techniques for transforming solids to the capsule form. Materials such as wheat, chemicals and others that must not come in contact with the carrying liquid can be encapsulated in thin metal or plastic containers. Minerals can be cast in the form of solid capsules. Yet another mode is to slightly extrude solid paste to form cylindrical capsules and transport these so-called paste slugs in a carrying fluid that is of substantially different nature than the liquid used for making the paste. An example is a paste slug formed from pulverized coal and oil and transported with water as the carrying medium. The high interfacial tension between water and oil keeps the slug together and this mode of transportation has also been found to have several other operational advantages (11).

1.1.3 Theoretical Developments

The experimental work at the Research Council of Alberta has stimulated some theoretical analysis of the capsule flow. Without exception, all the work has been focussed on the cylindrical capsule with an effective infinite length. Charles (12) and Kennedy (13) developed theoretical relationships for the velocity ratio and pressure gradient for a concentric flow of cylindrical capsules. Kruyer, Redberger and Ellis (14) carried out similar analysis for laminar eccentric flow of capsule for a known clearance between the capsule bottom and the pipe wall.

Garg and Round (15) suggested that the bottom clearance could be obtained from a force balance on the capsule if the pressure gradient is known. The procedure rests upon the supposition that the flow past a capsule can be described as the sum of pressure flow through the annulus due to the pressure gradient and Couette flow due to the drag force of the capsule wall. The method is applicable for both laminar and turbulent flow but its utility is limited since it involves complex numerical integration at least for the laminar flow. Moreover, they assume that the eccentricity is known. The reverse method for predicting pressure gradients from known velocity ratios has not been found to be very successful. The approach has been applied to the data of the Research Council of Alberta by Kruyer and Garg (16) with limited success.

The problem of capsule flow is exceedingly complex and does not seem to be amenable to a simple solution. However, an attempt to solve the problem in an integrated fashion utilizing all that we know so far about the capsule flow is expected to lead to some useful insights. An attempt on these lines is made in Chapter 3.

1.2 Experimental Set-Up

The experimental set-up used by the Research Council of Alberta is described fully in references (16) and (17). The exact arrangement varied somewhat with the different pipelines used to generate the data. Figure 1.1 shows a typical schematic representation of a horizontal straight shuttle pipeline that allows the shuttling back and forth of cylinderical capsules. Measurements are performed when the capsule travels through the test section. The capsule is inserted in a lock between valve 2 and 3 and is held stationary until the liquid attains steady state. The capsule is then injected into the flowing liquid by closing valve 3 and opening valve 2. It gathers momentum rapidly and only a short distance is needed to attain steady state capsule velocity. A four-way valve (V_1) determines the direction of liquid flow and two throttle valves (V_6, V_7) are used to control the flow rate.

Up to three centrifugal pumps can be used in parallel to provide a flow of 100 USGPM or liquid bulk velocities up to 8 feet/second. Pressure sensitive switches are provided for safety, generally set to turn off the pumps if the pressure exceeded 60 psi. Sensitive photo-cells also turned off the pumps before the capsule reached the pipe end to avoid shock to the pumps of sudden capsule stopping. A

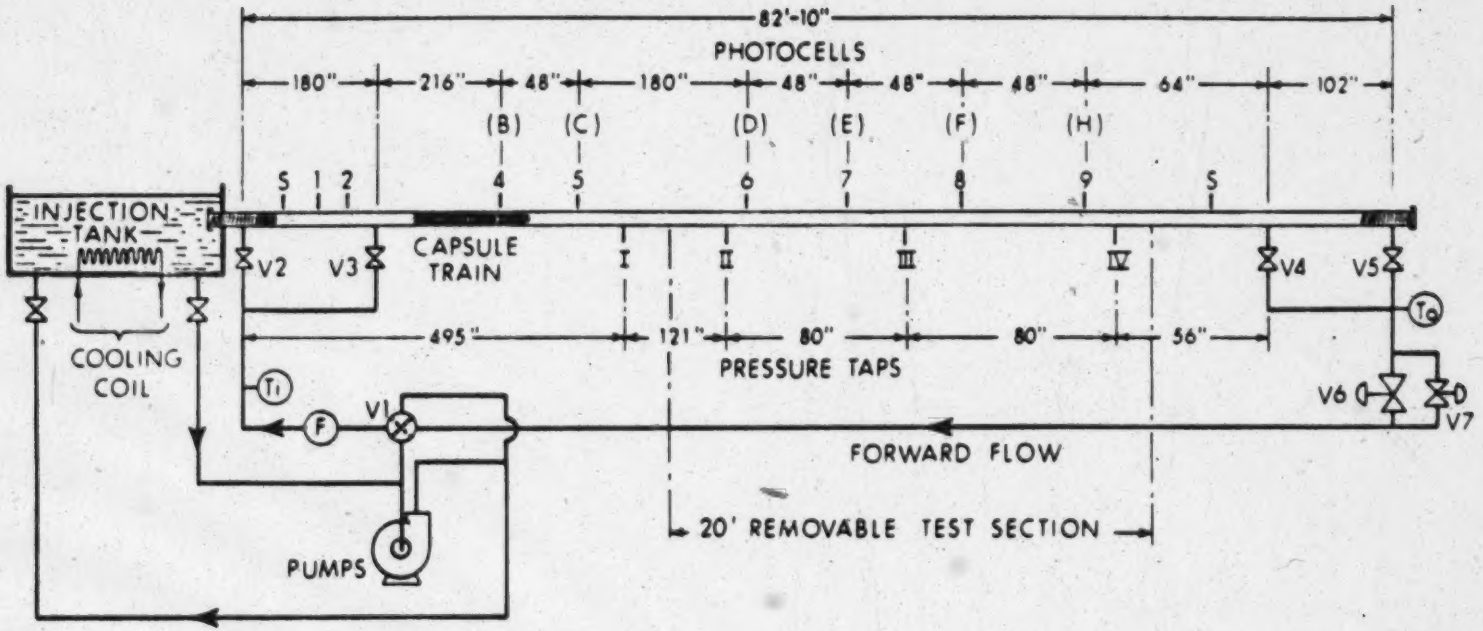

Figure I.1 Schematic illustration of 4-inch laboratory pipeline, Research Council of Alberta. (Courtesy J. Kruyer, Research Council of Alberta, Edmonton, Alberta)

cooling unit connected to a heat exchanger in the injection tank maintains temperature control within 2°F.

Variations in the internal pipe diameter in the test section can be kept within 0.01 in. except for the 10 in. line in which the maximum variation tolerated is 0.03 in. Capsule length can be kept constant within 0.05 in. and maximum variation in the capsule diameter can be held at 0.03 in. Capsule volumes and weight measurements allow the capsule densities to approach the selected densities within 0.5%.

A PDP-8-S (Digital Equipment Corporation) mini-computer is used for acquisition and partial processing of data. Figure 1.2 shows the flow of data and control information between the central processor and the equipment. The numbers near the top of the figure indicate how many channels were used to record the variable.

Temperatures are measured at the pipe inlet and outlet by thermistors that are regulated by a 1500 volt supply. The digitized voltage signal from the thermistors are fed to binary counters that are interfaced with the central processor. Pressure transducers used to measure pressure differentials also operate on a similar mechanism. The voltage from one of the pressure transducers can also be displayed on an oscilloscope to allow monitoring of the pressure differential.

The liquid flow is monitored by a magnetic flow meter and photocells are employed to detect the capsule. A crystal oscillator and a counter, interfaced with the central processor, are used to record time. Capsule velocities are measured to within 0.3% over the entire range and liquid flow rates are within 1%. The pressure transducers allow measurements to within 0.2% of the transducer range during calibration. Over a period of a month, however, the calibration error can be as much as 0.5%.

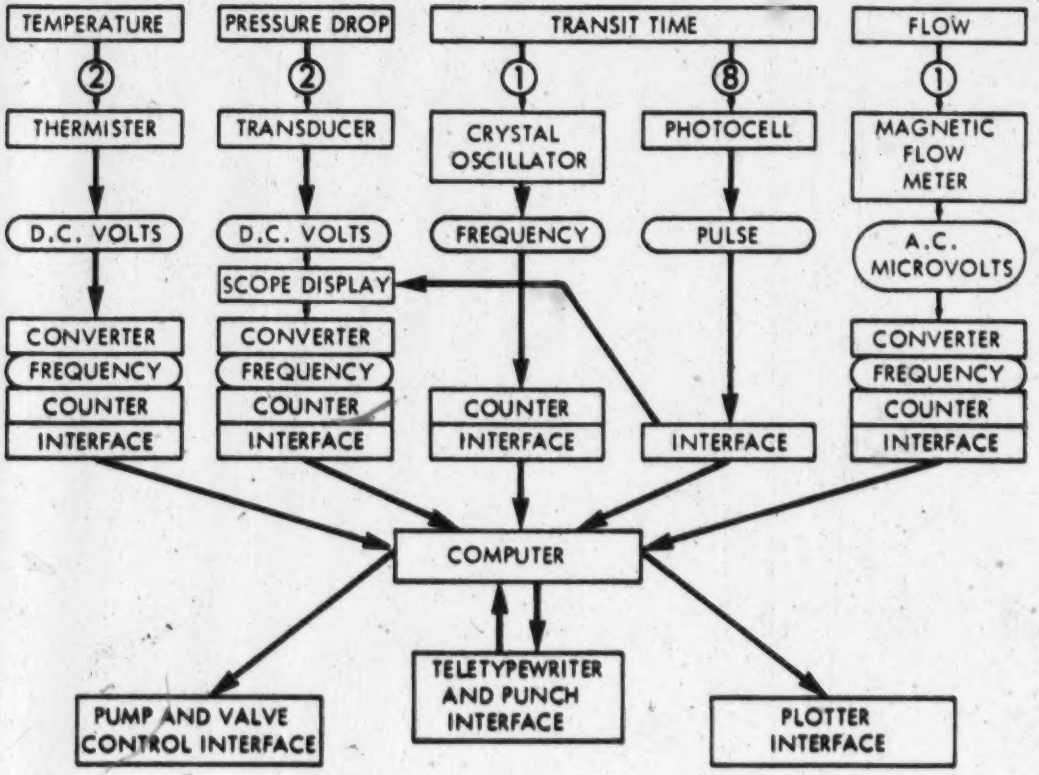

Figure I.2 Data flow diagram for the experimental set up, Research Council of Alberta (Courtesy J. Kruyer, Research Council of Alberta, Edmonton, Alberta)

A typical trace of pressure drop between the pipe taps as a capsule moves through the pipeline is shown in Figure 1.3. In a typical pass the capsule initially moves in the pipeline towards the first pressure tap so that the pressure differential is caused by the flowing liquid only. The trace of the pressure differential rises as the capsule moves past the first tap and becomes constant as the entire capsule length comes within the two pressure taps. The decline in the trace corresponds to the exit of capsule past the second tap. The average pressure differential is computed by numerical integration from the point D to H on the trace, i.e.

$$\text{Average } \Delta P = \Delta P_m = \frac{\int_D^H \Delta P \, dt}{\int_D^H dt} \tag{1.1}$$

where ΔP is the instantaneous pressure differential between the pressure taps and t is time. A similar integration is carried out for all the other variables. The pressure gradient for the capsule PGC can be obtained from the measured average pressure differential ΔP_m by the following formula:

$$PGC = [\Delta P_m - (L_p - L_c)\frac{\Delta P_f}{L_p}]/L_c \tag{1.2}$$

where L_p is the pipe length between the pressure taps, L_c is the capsule length and ΔP_f is the pressure differential for liquid flow alone.

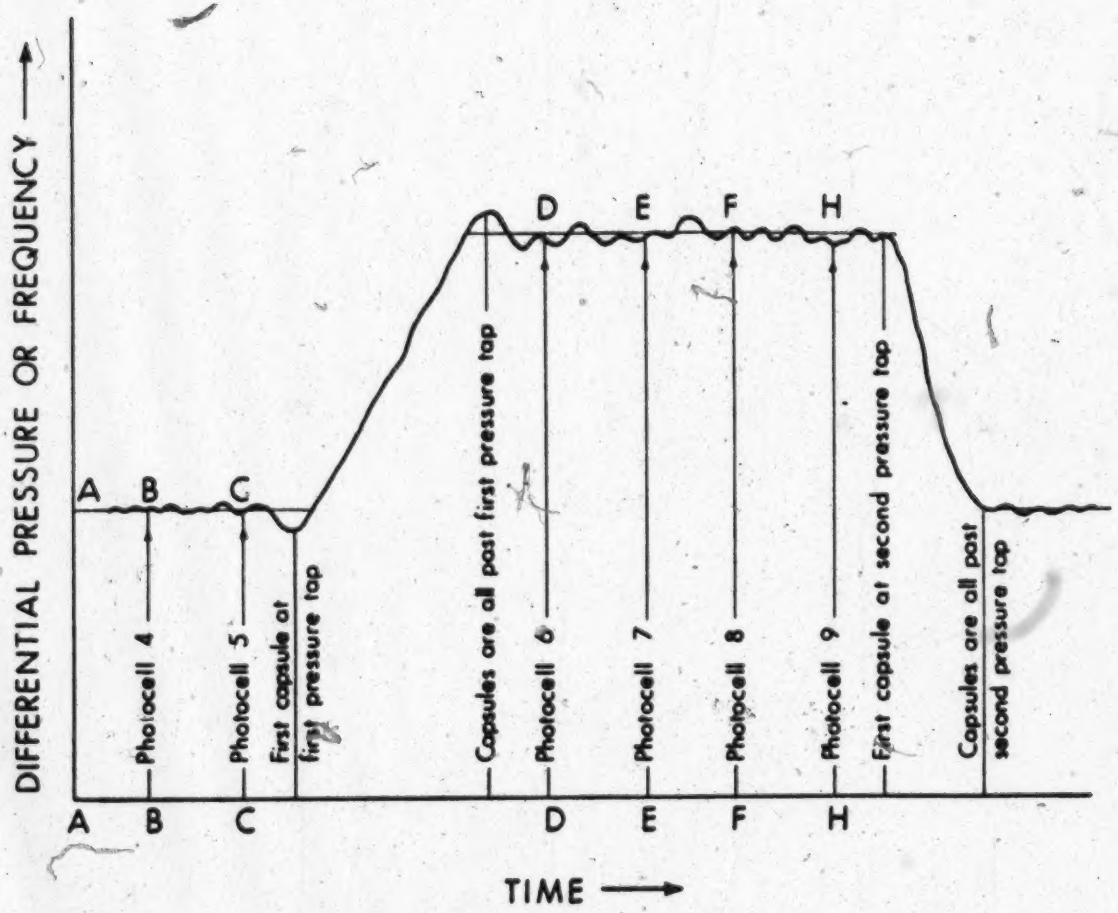

Figure 1.3 Trace of the pressure differential between taps in the capsule pipeline, Research Council of Alberta (Courtesy J. Kruyer, Research Council of Alberta, Edmonton, Alberta)

1.3 Model Discrimination and Model Building

1.3.1 Mathematical Modeling

A mathematical model is an abstract formulation aimed to simulate a real world phenomenon. A true mathematical model accounting completely for the physical phenomenon is a hypothetical concept and is seldom realized in non-trivial situations. Nevertheless, it is a useful tool for the scientists and engineers in representing the important characteristics of the actual methanism. One is often concerned with a situation where a dependent variable y, is related to a set of independent variables, $\underline{x} = \{x_1, x_2, \ldots x_r\}$. For example, an engineer might be studying the dependency of the pressure gradient y through a pipe on the pipe diameter x_1, the liquid viscosity x_2, the liquid density x_3, and others. Theoretically there exists a relation of the type

$$y = \phi(\underline{x}, \underline{a}) \tag{1.3}$$

between the dependent variable y and the set of independent variables $\underline{x}$, where $\underline{a} = \{a_1, a_2, \ldots a_r\}$ is the set of r parameters which may be the physical constants of the system under study. Usually, a simpler relation that closely approximates the outstanding fectures of (1.3) is satisfactory.

In the course of the modeling process, the analyst is faced with two classes of problems. One is an engineering situation where the purpose is to obtain a quantitative description of the process for design when extensive data are available in the region of interest. The "response surface" methodology deals with this class of problems and an empirical polynomial fit is usually satisfactory (18, 19, 20).

The other type of situation arises when the purpose is to establish the true nature of the process and several mechanistic models can be postulated. It is desired to discriminate among these rival mechanisms so as to identify the true mechanism. Here, the problems are twofold. In the first place, informative experiments have to be designed; secondly, the resulting data have to be analysed to discriminate among the rival model forms.

In the methodology to follow in the next chapter, a blend of the above two approaches has been employed. For the capsule flow problem, enough mechanistic insight is not available to warrant the later approach. Again, a purely empirical approach would require long and unwieldy polynomials since the number of independent variables is rather large. Semi-empirical models are generated on the basis of physical reasoning or merely intuitive judgement. In addition, some statistical tools are available for model improvements on an empirical basis.

1.3.2 Model Discrimination and Parameter Estimation

Once the models have been generated either empirically or mechanistically, discrimination among the rival model forms is carried out along Bayesian lines. The procedure follows that developed by D. Quon and the author (21, 22). Suppose we have m plausible model forms relating the dependent variable y to the set of independent variables $\underline{x}$, each model form ϕ_j containing a vector of parameters $\underline{a}_j$ of dimension r_j:

$$y = \phi_j(\underline{x}, \underline{a}_j) \qquad j = 1, \ldots, m \tag{1.4}$$

and n sets of experimental data, i.e. $\{y_i, \underline{x}_i: \ i=1, \ldots, n\}$.

If there is no prior information about the parameters in the region of interest then the prior parameter distribution is approximated by the improper uniform distribution which written in normal form is given by

$$f'(\underline{a}_j) = f_N(\underline{a}_j | \underline{\mu}_j, \underline{C}_j) \tag{1.5}$$

where $\underline{\mu}_j$ is any finite vector corresponding to the mean value for $\underline{a}_j$ and $\underline{C}'_j$, the prior variance covariance matrix, has infinite values along its diagonal.

The least squares estimate $\underline{a}_j$ is found by solving the following extremization problem:

$$\hat{S}_j^2 = \underset{a_j}{\text{Min}} \sum_{i=1}^{n} \{y_i - \phi_j(\underline{x}_i, \underline{a}_j)\}^2 = \sum_{i=1}^{n} \{y_k - \phi_j(\underline{x}_i, \hat{\underline{a}}_j)\}^2 \tag{1.6}$$

The algorithm for the parameter estimation is simple involving only a matrix inversion. Iterative convergent schemes have to be employed for models that are non-linear with respect to the parameters. Marquardt's (23) algorithm has been used for non-linear parameter estimation in this work.

The unbiased variance of fit is simply

$$\hat{\sigma}_j^2 = \frac{\hat{S}_j^2}{n - r_j} \tag{1.7}$$

and the design matrix for the j^{th} model

$$\underline{U}_j = \{\underline{u}_{ji}: \ i=1, \ \ldots \ n\} \tag{1.8}$$

where

$$\underline{u}_{ji} = \left\{ \left(\frac{\partial \phi_j}{\partial a_{jk}} \right)_{\substack{a_{jk} = \hat{a}_{jk} \\ \underline{x} = \underline{x}_i}} : k = 1, \ldots r_j \right\} \tag{1.9}$$

The information matrix is given by

$$\underline{A}_j = \frac{1}{\hat{\sigma}_j^2} \underline{U}_j^T \underline{U}_j \tag{1.10}$$

The posterior parameter distribution is now:

$$f''(\underline{a}_j) = f_N(\underline{a}_j | \hat{\underline{a}}_j, \hat{\sigma}_j^2 \underline{A}_j^{-1}) \tag{1.11}$$

For most purposes, it is adequate to assume that all the m models are equally likely before any experimental observations have been made. That is

$$p'(\phi_j) = \frac{1}{m} \tag{1.12}$$

The posterior probability of model form ϕ_j is obtained by using Bayes' theorem

$$p'(\phi_j) = \frac{p'(\phi_j)\, L(\underline{y}|\phi_j)}{\sum_{k=1}^{m} L(\underline{y}|\phi_k)} \tag{1.13}$$

where

$$L(\underline{y}|\phi_j) = \int_{\underline{a}_j} L(\underline{y}|\phi_j, \underline{a}_j)\, f''(\underline{a}_j)\, d\,\underline{a}_j$$

$$= \int_{\underline{a}_j} \prod L(y_i|\phi_j, \underline{a}_j)\, f''(\underline{a}_j)\, d\,\underline{a}_j \qquad (1.14)$$

$$= \int_{\underline{a}_j} \prod f_N(y_i|\phi_j(\underline{x}_i, \underline{a}_j), \sigma_j^2)\, f''(\underline{a}_j)\, d\,\underline{a}_j$$

The above integral has been evaluated in references (21, 22)

The posterior probability $p''(\phi_j)$ is used as a measure of the validity of the model form. It is a measure of the probability that the given model is the true model out of the set of models under consideration.

1.3.3 Tests of Model Adequacy

The posterior model probability is only a measure of the relative success of the given model in describing the data. When all the perceived models are poor ones, even the most successful may not be adequate for a given purpose. Simple tests of model adequacy have been developed in references (21) and (24) and may be summarized as follows:

a) The residual errors should be uncorrelated with all the independent variables. Existence of any such correlation suggests systematic modeling errors and that the model can be further improved.

b) The estimated error variance, as computed by relation (1.7) should not be larger than the experimental error variance, estimated on physical grounds. The variance of fit should not change drastically if various subsets of the data are employed or when additional data are incorporated.

c) The parameter estimates should not vary widely with the incorporation of additional data. Relatively stable parameter estimates over the entire operating space ensure that the model under consideration is general and not merely a 'local' approximation of some other intrinsic model form.

1.3.4 Model Improvement and Model Generation

If all the perceived models are found to be inadequate against the criteria of section (1.3.3), the models need to be improved by the addition and/or modification of some terms. Indeed, entirely new models might be necessary. However, there are no established procedures available for model generation or improvement. In dealing with the problem of the capsule flow, it was found that many of the models had to be generated on an ad hoc basis and most improvements were peculiar to the situations encountered. Some general guidelines in this regard that could be isolated from the experience with the capsule flow problem are given below.

a) Examine the correlation of the residual errors with each of the independent variables. If any regular trend in the errors is observed while examining against a particular variable x_j, then the model can be improved by modifying, adding or deleting the terms involving x_j.

b) The marginal variances of the parameter estimates (the diagonal elements of the variance covariance matrix) are useful in model simplification. A large parameter variance implies that the corresponding term may be safely dropped without significant deterioration in the model performance.

c) Graphical display of the dependent variables versus each of the independent variables can sometimes suggest the approximate functional dependency. Common mathematical functions for several values of the parameters may be plotted on the same scale as the actual data.

d) Simple transformation of the independent and dependent variables is a powerful tool for generating useful function groups. Among the common transformations are logarithmic, exponential, power and polynomial. Graphical display of the dependent variable with all other independent variables held constant, if such data are available, is usually sufficient to suggest a suitable transformation.

e) Semi-theoretical physical reasoning can help generate some useful model forms. The concept of driving force and resistance can be employed in examining the functional dependency. Some models may be discarded as being incongruous with the physics of the problem. Several others may be generated by modification of known models for the limiting cases (e.g. that of the concentric cylinders).

The capsule flow modeling problem has been attempted here through two different approaches. The first utilizes some of the theoretical insights based mainly on the experimental data and is described in Chapter 2. The alternate attempt while incorporating all the

important empirical observations is primarily a theoretical analysis of the capsule flow. The latter constitutes the subject matter of Chapter 3. The last chapter sums up the results of this work.

2. EMPIRICAL CORRELATIONS

2.1 Scope

In any engineering design involving the transportation of capsules in a pipeline, it is necessary to develop quantitative relationships between such key design variables as capsule velocity (which is directly related to pipeline capacity) and pressure drop and other parameters such as pipeline geometry, fluid properties, and the physical characteristics of the capsules. Unfortunately, the complexities of the flow phenomenon have frustrated any attempts up to now to develop a general theoretical mechanistic model that would describe and explain capsule pipeline flow. Consequently, we are reduced to formulating empirical correlations based on the extensive but by no means exhaustive data gethered over the past number of years, in particular, by the Research Council of Alberta. Difficulties are encountered even in developing empirical correlations. Thus while reasonably satisfactory capacity relationships will be presented in this chapter, no general satisfactory pressure drop correlation has been developed.

2.2 Physical Variables

Even a cursory physical analysis of capsule pipeline flow would indicate that at least the following independent variables might contribute to a complete specification of the flow system.

D pipe diameter, cm

d capsule diameter, cm

L_c capsule length, cm

S_c capsule end shape, dimensionless factor

σ capsule density, g/cc

ρ liquid density, g/cc

μ liquid viscosity, centipoise

V_b bulk liquid flow velocity in the pipe, ft/sec

E_p roughness factor of the pipe wall, dimensionless

E_c roughness factor of the capsule surface, dimensionless

Given the above, the following may be considered to be dependent or derived variables:

V_c capsule velocity, ft/sec

k ratio of capsule diameter to the pipe diameter d/D, dimensionless

V_{an} annulus velocity $(V_b-k^2V_c)/(1-k^2)$, ft/sec

VR velocity ratio V_c/V_b, dimensionless

PGF pressure gradient when liquid flows at the rate of V_b, psi

PGC pressure gradient for the capsule system, psi

PR pressure ratio PGC/PGF, dimensionless

ϵ minimum clearance between the capsule surface and pipe wall, cm

η coefficient of friction between the capsule surface and the pipe wall, dimensionless

ν kinematic viscosity of the liquid μ/ρ, centistokes

2.3 Experimental Data

Obviously not all the independent variables could be thoroughly investigated, nor could all the dependent variables be measured. In their experimental program, except for certain preliminary studies, the Research Council of Alberta concentrated on those ranges of parameter values which would most likely be encountered in industrial applications. The experimental procedure has been described in section 1.2. The ranges of conditions under which the Research Council of Alberta obtained data are summarized in Table 2.1.

Extensive runs were carried out for each different type of pipe and pipe size but the carrying liquid was either oil or water, thus limiting the range of liquid properties investigated. Both the diameter ratio and density of the capsules were varied over substantial ranges. All of the independent variables except E_p, E_c and S_c were measured. The roughness factors E_p and E_c had to be inferred; they may have changed during the course of experimentation, and such changes may indeed have been responsible for the apparent change in some of the pressure gradients to be noted later.
Of the dependent variables, the annulus velocity V_{an}, the clearance ε and the coefficient of friction η could not be measured.

2.4 Capacity Correlations

It was attempted to establish relationships of the type

$$V_c = f(V_b, D, k, \sigma, \rho, \nu, L_c/d, E_p, E_c, S_c) \qquad (2.1)$$

between the dependent variable V_c and the set of independent variables.

TABLE 2.1

DATA USED IN THIS WORK

Pipe Material	Pipe Diameter D	Capsule Description	Capsule Density σ	Capsule Diam. Pipe Diam. k	Kinematic Viscosity ν	Liquid Density ρ	No. of Runs	No. of Data Points
Copper	0.532	individual, 24" long, stainless steel	1.9-9.4	0.59-0.95	8-50	0.86	20	354
Copper	1.267	individual, 48" long, stainless steel	1.03-5.0	0.79-0.94	0.75	1.0	38	1776
Stainless Steel	4.026	trains of 4, 24" long, butyrate	0.99-5.0	0.69-0.95	10-30	0.84	14	448
Butyrate	4.026	trains of 4, 24" long, butyrate	0.75-3.0	0.87-0.96	1.06	1.0	36	616
Mild Steel	10.020	trains of 5, 48" long, mild steel	1.0-1.5	0.85-0.95	0.95	1.0	15	299
TOTAL	0.532-10.020		0.75-9.4	0.59-0.96	0.7-50	0.84-1.0	123	3493

For any given run, all the independent variables except V_b have been held constant. The first step towards identifying the relation (2.1) was to model all the individual runs for each pipe size. Among others, the following models were considered to fit the data of individual runs:

Model 1

$$VR = \frac{C_1 V_b}{(1 + C_2 V_b^{C_3})} \tag{2.2}$$

Model 2

$$V_c = b_1 + b_2 V_b^{b_3} \tag{2.3}$$

where c_1, c_2, c_3, b_1, b_2 and b_3 are functions of D, k, σ/ρ, ν, L_c/d, E_p, E_c and S_c. Since these independent variables have constant values for a given run, the parameters c_1, c_2, c_3, b_1, b_2, and b_3 can be uniquely estimated for each run. Model 1 was formulated from the shapes of VR versus V_c plots and model 2 was inferred from V_b versus V_c plots for individual runs.

Fitting models 1 and 2 to the data of several sample runs resulted in the lower variance of fit for model 2 in all cases. Furthermore, model 1 was found to be inadequate when tested against the criteria of section 1.3:

1) Widely varying estimates of parameters depending upon the region of the subset of data used; e.g., low V_b or high V_b region.
2) Estimated variance of fit was found to be dependent upon the number of data points used in a given subset and the region of data in the given subset.

Model 2, on the other hand resulted in relatively stable parameters and variance estimates. Furthermore, it could be inferred from parameter estimates of only a few sample runs that within 95% confidence limits, $b_3 = 1$. Table 2.2 gives the values of the parameter b_3 and its 95% confidence limits for some sample runs. A newly acquired APL plot subroutine (Appendix G) was used to detect any curvature in the remaining runs and fairly good straight lines were obtained. This obviated the need for testing the remaining runs by an extensive non-linear search for the parameter b_3. Figure 2.1 shows the plot of V_c versus V_b for a typical run.

Model 2 was thus simplified to

$$V_c = b_1 + b_2 V_b \tag{2.4}$$

where $$b_1 = f_1(k, D, \sigma/\rho, \nu, L_c/d, E_p, E_c, S_c) \tag{2.5}$$

and $$b_2 = f_2(k, D, \sigma/\rho, \nu, L_c/d, E_p, E_c, S_c) \tag{2.6}$$

The correlation (2.4) described accurately 99% of the experimental data within $\pm$ 1% of the average value for most of the runs and within $\pm$ 5% for all the runs. Table 2.3 shows the parameter and variance estimates from the data on the 1 1/4" copper pipeline.

The next step was to identify the functional dependence of b_1 and b_2 on the remaining independent variables. A few preliminary runs indicated that the capsule end shape factor S_c and the capsule length to diameter ratio L_c/d did not materially affect the parameters b_1 and b_2 for L_c/d greater than about 6 (5). Unfortunately, the effect of pipe diameter could not be isolated since each pipe

TABLE 2.2

ESTIMATES OF b_3 FOR SAMPLE RUNS
IN 1 1/4" COPPER PIPE LINE

Run No.	b_3	95% Limits
428	1.003	$\pm$ .011
429	.989	.010
412, 413	.987	.004
421	.977	.007
452	.995	.188
447	.929	.231
446	1.073	.106
441	.993	.003
440	.994	.004
408	1.002	.003
416	1.005	.003

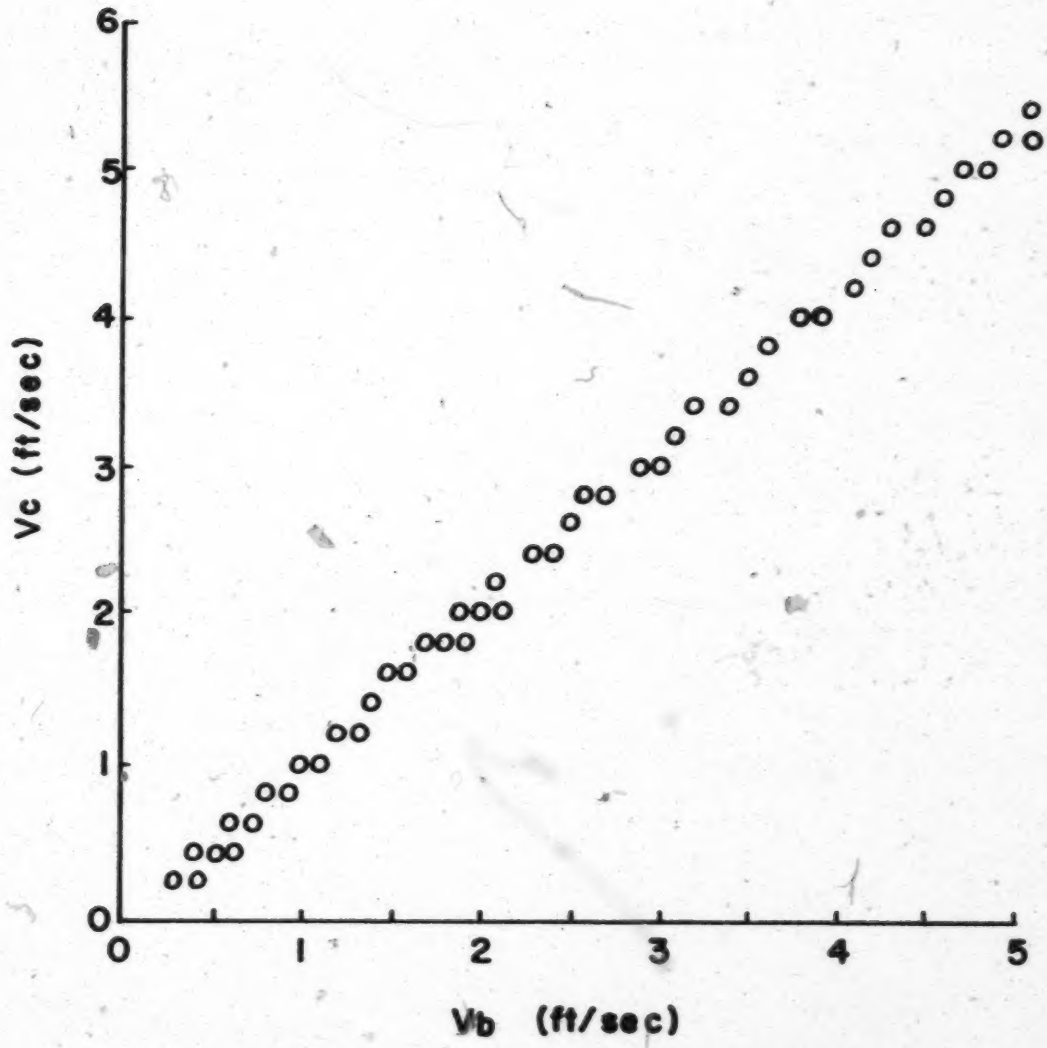

Figure 2.1 Vc versus Vb for run # 424, 1 1/4" copper line carrying steel capsules, Research Council of Alberta.

TABLE 2.3

PARAMETERS AND VARIANCE ESTIMATES
FOR 1 1/4" COPPER PIPE LINE

Run No.	σ	k	b_1	b_2	σ_*^2
408	1.031	.94	-.03105	1.05960	1.91×10^{-5}
410	1.031	.8895	-.06898	1.11423	6.88×10^{-5}
412+413	1.032	.839	-.19789	1.17697	8.62×10^{-5}
414	1.031	.7916	-.27800	1.22815	1.93×10^{-4}
416	1.125	.94	-.04387	1.06434	3.91×10^{-5}
418	1.125	.8895	-.19648	1.13260	8.82×10^{-5}
420+421	1.125	.839	-.45320	1.2077	2.63×10^{-4}
422	1.125	.7916	-.73872	1.27162	3.38×10^{-4}
424	1.25	.94	-.09543	1.06725	6.31×10^{-5}
426	1.25	.8895	-.33449	1.1457	1.80×10^{-4}
428+429	1.25	.839	-.69178	1.2175	2.44×10^{-4}
430	1.25	.7916	-1.44900	1.3066	2.34×10^{-3}
432	1.5	.94	-.17152	1.07468	3.09×10^{-5}
434	1.5	.8895	-.51370	1.1682	6.41×10^{-5}
436+437	1.5	.839	-.89606	1.23461	4.94×10^{-4}
438	1.5	.7916	-1.72840	1.34691	5.52×10^{-4}
440+441	2.0	.94	-.30188	1.08865	5.56×10^{-5}
442	2	.8895	-.76826	1.157783	6.84×10^{-4}
444+445	2	.839	-1.38076	1.2117848	7.16×10^{-3}
446+447	2	.7916	-2.3261	1.328178	1.50×10^{-2}
448	3	.94	-.41845	1.08540	1.15×10^{-4}
450	3	.8895	-1.0493	1.16786	7.51×10^{-3}
452+453	3	.839	-2.2445	1.27304	1.90×10^{-2}
454	3	.7916	-3.51224	1.44130	3.79×10^{-3}
456	5	.94	-.57372	1.07729	1.44×10^{-3}
458	5	.8895	-1.85227	1.18449	1.20×10^{-2}

diameter was associated with a different pipe material (with variation in E_p) or with a different capsule material (with variation in E_c). Therefore, the best that could be done was to obtain the functional forms for the parameters b_1 and b_2 for each experimental pipeline rather than a general correlation covering all the pipelines.

Thus

$$b_1 = \phi_p(k, \sigma/\rho, \nu) \tag{2.7}$$

$$\simeq \phi_1(k, \sigma/\rho)\phi_2(\nu) \tag{2.8}$$

and

$$b_2 = \psi_p(k, \sigma/\rho, \nu) \tag{2.9}$$

$$\simeq \psi_1(k, \sigma/\rho)\psi_2(\nu) \tag{2.10}$$

The functional forms ϕ_p and ψ_p now characterize the specific pipeline size, the pipe material and the capsule material. The factorization of the functional forms in (2.8) and (2.10) implies independence of the effects due to capsule/pipe diameter ratio and capsule density on the one hand and liquid viscosity on the other. There is no theoretical justification for the factorization but for the two pipelines in which viscosity was varied, the use of the empirically best forms for ϕ_2 and ψ_2, i.e.

$$\phi_2 = \frac{1}{\nu^{0.25}} \tag{2.11}$$

$$\psi_2 = \nu \tag{2.12a}$$

or

$$\psi_2 = 1 \tag{2.12b}$$

gave satisfactory correlations. In the other pipeline data, the range of viscosity variation was not sufficient to test the validity of the assumption.

The functions ϕ_1 and ψ_1 were found to be more complicated and no single model was successful for all the pipelines, suggesting that any functional forms not including surface roughness could only give locally correct predictions. The technique used for selecting models and estimating parameters follows along the Bayesian lines described in section 1.3. For preliminary modeling of ϕ_1 and ψ_1, the parameter estimates b_1 and b_2 from individual runs were used. The model formulation and evaluation consisted of examination of plots, residual errors, variance of fit and application of logarithmic and power transformation of variables.

To keep the analysis tractable and the resulting functional forms simple, only single term functional forms were investigated. One of the powerful tools for generating model forms employed was semi-theoretical reasoning. For example in determining the functional form of b_2 for laminar flow:

$$\text{Resistance to flow} \propto \frac{1}{(\text{clearance} = 1-k)^c}$$

$$\propto \text{surface area of capsule } k$$

$$\text{or the two surface areas } (1+k)$$

$$\text{Driving force} \propto \text{cross sectional area } k^2$$

$$\propto V_b$$

$$\text{So that} \quad V_c \propto \frac{\text{Driving force}}{\text{Resistance}}$$

$$\propto \frac{(1-k)^c\ k^2}{(1+k)} V_b$$

Thus $$b_2 = \frac{k^2(1-k)^c}{(1+k)}$$

where c is an arbitrary power to be determined from the use of data.

As an example, Tables 2.4 and 2.5 give some of the model forms tried for ϕ_1 and ψ_1 using parameter estimates b_1 and b_2 from the data of 1 1/4" copper line carrying steel capsules. Some of the more successful forms for ϕ_1 and ψ_1 as determined from this preliminary examination were then incorporated in the overall capacity model

$$V_c = \phi_{1,p}(k, \sigma/\rho)\phi_{2,p}(\nu) + \psi_{1,p}(k, \sigma/\rho)\psi_{2,p}(\nu)V_b \qquad (2.13)$$

where the subscript 'p' refers to a given pipe-capsule system.

All available raw data for the given pipe were used for parameter estimation and to evaluate the performance of the overall capacity model. The most successful relations obtained for each pipe along with the variance of fit σ_*^2 and the 95% limits of the predictions from these relations are given in Table 2.6. The 95% confidence limits ($\pm\ell$) can be interpreted in either of the two ways, viz., that the given correlation generates 95% of the data within the accuracy limits of $\pm\ell$ or one can be 95% confident that a prediction made by a given correlation is correct within $\pm\ell$. This of course assumes that the prediction is made within the region spanned by the data.

To simplify the presentation in Table 2.6 we define:

$$K1 = (1-k)$$

$$K2 = (1-k^2)\left(\frac{|\sigma-\rho|}{\sigma}\right)$$

TABLE 2.4

MODELING FOR ϕ_1 FOR 1 1/4" COPPER LINE

CARRYING CYLINDERICAL STEEL CAPSULES

Model Form	Variance of fit σ_*^2	Parameters C_1	C_2
$C_1(\frac{\sigma}{\sigma+\rho})(1-k^2)^2$	.3022	-21.5	
$C_1 \ln(\frac{\sigma}{\rho})(1-k^2)^2$	.03953	-24.59	
$C_1 \ln(\frac{\sigma}{\rho})(1-k)$	.129	-13.1	
$C_1 \ln(\frac{\sigma}{\rho})(1-k^2)$	.149	- 7.05	
$C_1 \ln(\frac{\sigma}{\rho})(1-k)^2$	.043	-81.1	
$C_1 \ln(\frac{\sigma}{\rho})(1-k^4)$	.190	- 4.04	
$C_1 \ln(\frac{\sigma}{\rho})\frac{(1-k^2)}{(1+k^2)}$	.114	-12.19	
$C_1 \ln(\frac{\sigma}{\rho})\frac{(1-k^2)^2}{(1+k^2)^2}$	.0486	-68.06	
$C_1 \ln(\frac{\sigma}{\rho})\frac{(1-k^2)^2}{(1+k^2)}$	.0423	-40.99	
$C_1 \ln(\frac{\sigma}{\rho})(1-k)^4$	1.228	-20.40	
$C_1(\frac{\sigma-\rho}{\sigma})(1-k)$	.0832	-20.80	
$C_1 \ln(\frac{\sigma+\rho}{\sigma})(1+k^2)^2$	1.126	- .386	
$C_1(\frac{\sigma}{\sigma+\rho})(1+k^2)^2$	.757	- .44	
$C_1(\frac{\sigma-\rho}{\sigma})(1-k^2)^2$	.0302	-37.604	

(Continued)

TABLE 2.4

(Continued)

Model Form	Variance of Fit σ_*^2	Parameters C_1	C_2
$C_1(\frac{\sigma}{\sigma+\rho})(1-k^2)^2$	.302	-21.5	
$C_1(\frac{\sigma-\rho}{\sigma})(1-k^2)^2(1+k)$	.0285	-20.72	
$C_1(\frac{\sigma-\rho}{\sigma})(1-k^2)^2(1+1)^2$	.02789	-11.404	
$C_1(\frac{\sigma-\rho}{\sigma})(1-k^2)(1-k^4)$	.02785	-22.56996	
$C_1(\frac{\sigma-\rho}{\sigma})^{C_2}(1-k^2)(1-k^4)$	.02689	-21.9835	.9590
$C_1(\frac{\sigma}{\rho})^{C_2}(1-k^2)(1-k^4)$	.0495	3.7	1.25
$C_1(\frac{\sigma-\rho}{\rho})(1-k^2)(1-k^4)$	.1325	- 8.05	

TABLE 2.5

MODELING OF ψ_1 FOR 1 1/4" COPPER LINE

CARRYING CYLINDERICAL STEEL CAPSULES

Model Form	Variance of Fit σ_*^2	Parameters d_1	d_2
$d_1(\frac{1}{k})(\frac{\sigma}{\rho})^{d_2(1-k)}$	.00044	.996	.4540
$d_1(\frac{1}{k})(\frac{\sigma}{\rho})^{d_2(1-k^2)}$	.00047	.996	.2458
$1 + d_1(\frac{1}{k} - 1)(\frac{\sigma}{\rho})^{d_2(1-k^2)}$	.000317	.9977	1.199
$1 + d_1(\frac{1}{k} - 1)(\frac{\sigma}{\rho})^{d_2(1-k)}$	.000319	.99919	2.1605
$1 + d_1(\frac{1}{k} - 1)(\frac{\sigma}{\rho})^{d_2(\frac{1}{k} - 1)}$	.000328	1.0033	1.7216
$1 + d_1(1-k)(\frac{\sigma}{\rho})^{d_2(\frac{1}{k} - 1)}$	.000310	1.19945	1.86473
$1 + d_1(1-k^2)(\frac{\sigma}{\rho})^{d_2(\frac{1}{k} - 1)}$	.00037	.65	1.94
$1 + d_1(1-k)(\frac{\sigma}{\rho})^{d_2(1-k)}$	.000353	1.196	2.307
$1 + (\frac{1}{k} - 1)(\frac{\sigma}{\rho})^{d_1(1-k)}$	.000325	1.9937	
$1 + d_1 \frac{(\frac{\sigma}{\rho})^{d_2(1-k)}}{[\frac{7}{4}k(1-k) + \frac{49}{60}(1-k)^2 + k^2]}$	.00458	1.098	.694
$\frac{d_1(\frac{\sigma}{\rho})^{d_2(\frac{1}{k} - 1)}}{[\frac{7}{4}k(1-k) + \frac{49}{60}(1-k)^2 + k^2]}$	.0041	1.096	.612

Table 2.5 Continued

TABLE 2.5
(Continued)

$1 + d_1(1-k)(\frac{\sigma-\rho}{\rho})^{d_2(1-k)}$	.00067	1.611	.6244
$1 + d_1(1-k)(\frac{\sigma-\rho}{\sigma})^{d_2(1-k)}$	.000955	1.7195	.6744
$1 + d_1(1-k^2)(\frac{\sigma-\rho}{\sigma})^{d_2(1-k)}$	.000913	.875	.603
$1 + d_1(1-k)(\frac{\sigma-\rho}{\rho})^{d_2(1-k^2)}$	.00066	1.612	.3459

TABLE 2.6

SUMMARY OF THE CAPACITY CORRELATIONS

Pipe	Correlation	σ_*^2	95% Limits ($\pm\ell$) ft/sec
1/2" copper	$V_c = 0.02368\ \nu\ V_b$	0.001329	$\pm$ 0.073
1 1/4"copper	$V_c-V_b = -31.79(K4)(1+0.55(S1)k) + 1.159(K1)(K6)V_b$	0.006899	$\pm$ 0.166
	$V_c-V_b = -32.01(K4)-17.37(K4)(S1)k + 1.159(K1)(K6)V_b$	0.006902	$\pm$ 0.166
	$V_c-V_b = -37.06(K4)(1+0.4(S1)k) + 1.153(K1)(K6)V_b$	0.0719	$\pm$ 0.170
4" steel	$V_c-V_b = -14.21\ \frac{K5}{\nu^{0.25}} - 3.208\ \frac{K5}{\nu^{0.25}}(S2) + 0.08448\ V_b$	0.0117	$\pm$ 0.216
4" plastic	$V_c-V_b = -30.21(K3) + 1.118(S1)k + 0.845(K1)V_b + 2.378(K1)^2\left\|\frac{\sigma-\rho}{\sigma}\right\|V_b$	0.01234	$\pm$ 0.222
10" steel	$V_c-V_b = -1.591(K3)(1+k)^2(1+4.35(S1)k) + 0.6972(\sigma/\rho)^{2.6K1}\ V_b$	0.01478	$\pm$ 0.243
	$V_c-V_b = -27.12(K3)(1+0.4(S1)k) + 0.6814(K1)\ V_b$	0.01801	$\pm$ 0.268

$$K3 = (1-k^2)(1-k^4)\left(\frac{|\sigma-\rho|}{\sigma}\right)$$

$$K4 = (1-k^2)(1-k)\left(\frac{|\sigma-\rho|}{\sigma}\right)$$

$$K5 = (1-k^2)^{3/2}\left(\frac{|\sigma-\rho|}{\sigma}\right)$$

$$K6 = \left(\frac{\sigma}{\rho}\right)^{2.3(1-k)}$$

$$S1 = |\sigma-0.8\rho| + \frac{1}{|\sigma-0.8\rho|}$$

$$S2 = \left|\frac{\sigma}{\rho} - k\right| + \frac{1}{\left|\frac{\sigma}{\rho} - k\right|}$$

where $|\sigma-\rho|$ = absolute value of $(\sigma-\rho)$.

2.5 Towards a General Correlation

A general capacity correlation that is valid over a wide range of viscosities and pipe diameters would be of utmost practical importance. Although such a correlation could not be obtained, a general model form has been evolved in the following few pages.

2.5.1 Dimensional Analysis

The relation

$$V_c = f(V_b, D, d, \sigma, \rho, \nu, L_c, \eta, g)$$

may be approximated by

$$V_c = \sum_{i=1}^{n} V_b^{x_{1i}} D^{x_{2i}} d^{x_{3i}} \sigma^{x_{4i}} \rho^{x_{5i}} L_c^{x_{6i}} \nu^{x_{7i}} g^{x_{8i}} \eta^{x_{9i}} \quad (2.14)$$

where n is a suitable integer number and $x_{1i}, x_{2i}, \cdots x_{9i}$ are arbitrary constants. Now, each term on the right hand side of (2.14) must have

the dimensions of V_c. Dropping the second subscript 'i' for convenience,

$$[V_c] = [V_b]^{x_1} [D]^{x_2} [d]^{x_3} [\sigma]^{x_4} [\rho]^{x_5} [L_c]^{x_6} [\nu]^{x_7} [g]^{x_8} [\eta]^{x_9} \quad (2.15)$$

where [Z] represents the dimensions of Z. Thus

$[V_b] = [V_c] = LT^{-1}$ $\qquad$ $[L_c] = [d] = [D] = L$

$[\nu] = T^{-1}L^2$ $\qquad$ $[\sigma] = [\rho] = ML^{-3}$

$[g] = LT^{-2}$ $\qquad$ $[\eta]$ = dimensionless

The solution of (2.15) obtained by balancing the three fundamental dimensions of M, L and T is

$$x_5 = -x_4$$

$$x_1 = 1 - x_7 - 2x_8$$

$$x_2 = -x_3 - x_6 - x_7 + x_8$$

Therefore (2.15) can be rewritten as

$$V_c = V_b \left(\frac{V_b D}{\nu}\right)^{-x_7} \left(\frac{V_b^2}{Dg}\right)^{-x_8} \left(\frac{d}{D}\right)^{x_3} \left(\frac{L_c}{D}\right)^{x_6} \left(\frac{\sigma}{\rho}\right)^{x_4} \eta^{x_9} \quad (2.16)$$

or generally

$$V_c = \sum_{i=1}^{n} V_b \left(\frac{V_b D}{\nu}\right)^{a_{1i}} \left(\frac{\nu V_b}{D^2 g}\right)^{a_{2i}} \left(\frac{\sigma}{\rho}\right)^{a_{3i}} \left(\frac{L_c}{D}\right)^{a_{4i}} \eta^{a_{5i}} \left(\frac{d}{D}\right)^{a_{6i}} \quad (2.17)$$

where $a_{1i}, a_{2i}, \cdots a_{6i}$ are determined by $x_{1i}, \cdots x_{9i}$.

2.5.2 Incorporating Empirical Observations

Relation (2.17) has been obtained from purely dimensional considerations. Empirical information is now needed to simplify this large equation. We know from the results of section 2.4 that the successful capacity correlation should be of the form

$$V_c = b_1\phi_1(k, \sigma/\rho, L_c/D, \eta) + b_2\phi_2(k, \sigma/\rho, L_c/D, \eta)V_b + b_3\phi_3(k, \sigma/\rho, L_c/D, \eta)\nu V_b \quad (2.18)$$

or $$V_c = b_1 \frac{\phi_1}{\nu^{0.25}} + b_2\phi_2 V_b + b_3\phi_3\nu V_b \quad (2.19)$$

Furthermore

1) The second term may also be a function of viscosity. We do not have enough viscosity variations in the data to confirm or reject this hypothesis.
2) For the 1/2" line, with high ν, the first two terms of (2.18) practically vanish.
3) For other lines of higher D and lower ν, the last term is not significant.

A form of (2.17) that is consistent with all the empirical observations noted above is

$$V_c = b_1 V_b \left(\frac{\nu}{V_b D}\right)^{a_1} \left(\frac{D^2 g}{\nu V_b}\right)^{1-a_1} \phi_1 + b_2 \left(\frac{D^3 g}{\nu^2}\right)^{a_2} \phi_2 V_b$$

$$+ b_3 \left(\frac{\nu^2}{D^3 g}\right)^{1/2} \phi_3 V_b$$

$$= b_1 D^{2-3a_1} g^{1-a_1} \nu^{2a_1-1} \phi_1 + b_2 \left(\frac{D^3 g}{\nu^2}\right)^{a_2} \phi_2 V_b$$

$$+ b_3 \frac{\phi_3}{D^{3/2} g^{1/2}} \nu V_b \qquad (2.20)$$

where $a_2 > 0$ and $a_1 < 0.5$ and

$$[\phi_1 = \phi_1(k, \sigma/\rho, L_c/D, \eta)]$$

Furthermore, we know that

$$\phi_1 = K3(1 + C_1 S_1 k) f_1(\eta) \qquad (2.21)$$

or $$\phi_1 = (K4)(1 + C_1 S_1 k) f_1(\eta)$$

$$\phi_2 = 1 + C_2(1-k)\left(\frac{\sigma}{\rho}\right)^{C_3(1-k)} f_2(\eta) \qquad (2.22)$$

or $$\phi_2 = 1 + C_4(1-k^2)\left(\frac{\sigma-\rho}{\rho}\right) f_2(\eta)$$

$$\phi_3 = f_3(\eta) \qquad (2.23)$$

where C_1, C_2, C_3 and C_4 are positive constants and f_1, f_2, f_3 are suitable functional forms.

2.5.3 Flow Regimes

What is the dimensionless number that determines the nature of relationship between V_c and V_b? We have at least two different flow regimes corresponding to the relations (2.12a) and (2.12b). One physical quantity that apparently does affect the relationship is the viscosity of the carrying fluid.

To explore the problem further, the following empirical analysis was carried out. From the available data for the 4" steel line, certain data points having the following characteristics were selected

$$\nu > 19 \text{ c.s.}$$

$$V_b < 1.0 \text{ ft/sec.}$$

These conditions ensured that the apparently defined Reynolds numbers $V_b D/\nu$ for the selected data were well within the range of Reynolds numbers for the 1/2" line data. These selected points did not fit the best correlation for 1/2" line very well ($\sigma_*^2 = 0.0421$ as against $\sigma_*^2 = 0.00133$ for the entire 1/2"line). This suggests that the Reynolds number does not determine the nature of the capacity correlation. Furthermore, these selected 30 points correlated quite well with the most successful model for the 4" steel line. Table 2.7 compares the results of parameter estimation for the small subset of data containing only the low velocity and high viscosity points against those obtained from all the data.

Considering that the low velocity data cover an extremely small range, the agreement of the parameter estimates in Table 2.7 is quite satisfactory. Thus, it may be concluded that the model under consideration is a reasonable approximation to the true relationship. Moreover, it

TABLE 2.7

MODEL PERFORMANCE FOR LOW VELOCITY DATA
FOR 4" STEEL LINE

$$V_c - V_b = b_1 \frac{K5}{\nu_{0.25}} + b_2 \frac{K5\ S2}{\nu_{0.25}} + b_3 V_b$$

	Low Velocity 30 Data Points	All 448 Data Points
σ_*^2	0.004773	0.0117
b_1	$-19.71 \pm 2.749^+$	$-14.21 \pm 0.6337^+$
b_2	-3.964 ± 0.5844	-3.208 ± 0.1937
b_3	0.2997 ± 0.0961	$0.08448 \pm .00484$

$^+$95% confidence limits.

also implies that the nature of relationship between V_c and V_b is independent of V_b. Hence the dimensionless number that would determine such a relationship should not contain V_b. A dimensionless number that contains ν and D but not V_b is

$$S = \left(\frac{D^3 g}{\nu^2}\right) \tag{2.24}$$

This number has been defined as the Galileo number* but we will call it the stationary number since it is independent of the fluid velocity. We have seen the introduction of the stationary number to make the terms of (2.20) consistent with the experimental observations. As an example, for the 1/2" line

$$\nu \simeq 40 \text{ cs.}$$

$$D = 1.3 \text{ cm}$$

$$g = 981 \text{ cm/sec}^2$$

thus $$S \simeq 10^4.$$

Table 2.8 gives the stationary number for the various pipelines whose data have been used in this work. We know that for 1/2" line with $S \simeq 10^4$, the capacity correlation is of the type

$$V_c = b_1 + b_2 \nu V_b$$

and for other lines with $S > 3 \times 10^7$ the correlations are of the type

$$V_c = b_1 + b_2 V_b$$

where b_2 is not a function of ν. However, there is too wide a gap between the two values which can only be investigated through further experimentation.

---

*c.f. Chem. Eng. Progress 55, No. 9, p. 57 (Sept. 1959).

TABLE 2.8

STATIONARY NUMBERS FOR VARIOUS LINES

Pipe Line	S
1/2" copper	1×10^4
1 1/4" copper	5×10^8
4" Steel	3×10^7
4" Plastic	1×10^{10}
10" steel	1×10^{11}

A note of caution seems appropriate at this stage regarding the role of the stationary number as a determinant of capacity correlations. An equally important and perhaps even dominant factor is the capsule/pipe friction factor η. Again, the only way to identify the effects of each factor (stationary number on the one hand and η on the other) separately is through experimental data.

Furthermore, the stationary number does not characterize the flow mechanism of the capsule system. All that is implied in the foregoing section is that V_c and V_b follow the same relationship and both increase similarly with the changing mechanism of flow as V_b increases. Thus, S cannot be used to determine the relationship between PGC and V_b.

2.6 Pressure Gradients

The same model building techniques were used to try and obtain pressure drop correlations. However, no correlation could be established that was general enough to be of any practical utility. Part of the difficulty resulted from the relatively more complex nature of the pressure drop model, but most of the difficulty arose from the change in experimental conditions from run to run, the explanation of which will be suggested later.

An examination of several typical plots of PGC versus V_b such as in Figures 2.2 and 2.3, suggests very strongly that some other uncontrolled parameter has a much greater effect on PGC than V_b. That other parameter could be the surface conditions of the capsule and of the pipe. This subject will be further explored in the next chapter.

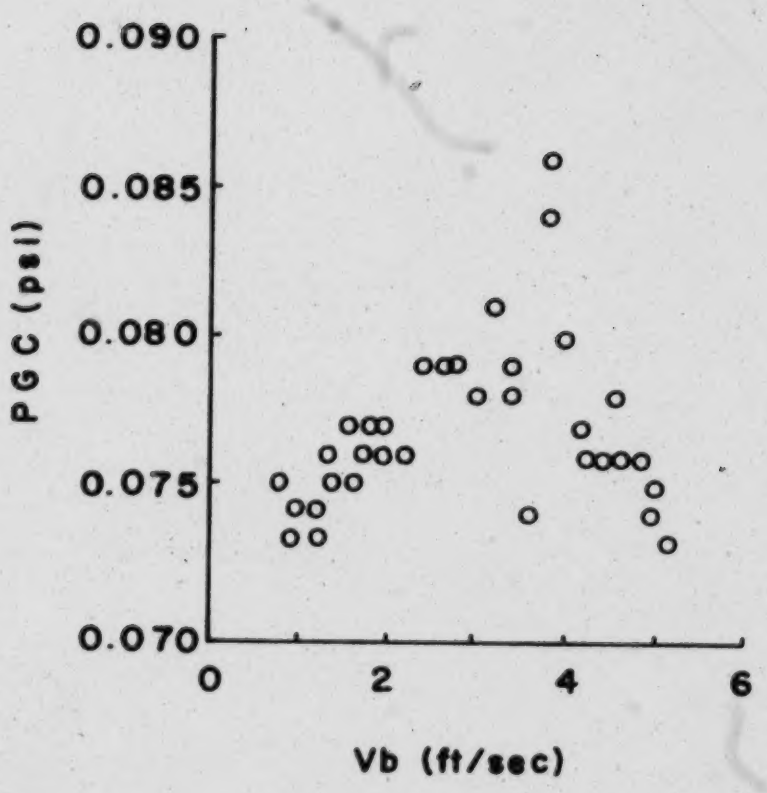

Figure 2.2 PGC versus Vb for run # 436 1 1/4" copper line carrying steel capsules in water, Research Council of Alberta.

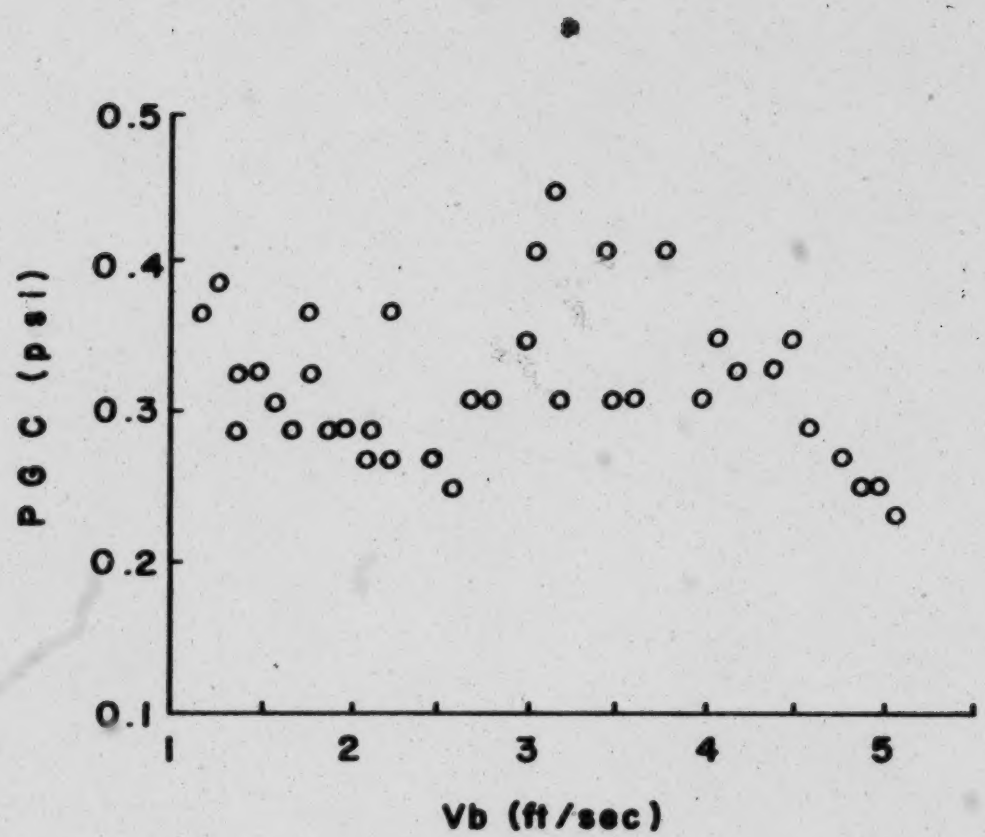

Figure 2.3 PGC versus Vb for run # 450, 1 1/4" copper line carrying steel capsules in water, Research Council of Alberta.

Fitting the data of a few experimental runs to the following simple smoothing models provided an estimate of measurement variance for the pressure gradients.

$$PGC = b_1' + b_2' V_b \tag{2.25}$$

$$PGC = b_1'' + b_2'' V_b + b_3'' V_b^2 \tag{2.26}$$

Table 2.9 gives the lower of the two variance estimates for 1 1/4" copper line carrying steel capsules. It can be seen that measurements are becoming more and more uncertain as σ increases and k decreases. Compared to the small range of PGC, the errors are large. These errors may be tolerable for an individual run but when the estimates of the parameters from these runs have to be modeled in terms of k and σ, one might end up with a totally inadequate or even misleading model. For most of the pipe lines, even a qualitative relationship could not be obtained between the shape of PGC versus V_b and k and σ. This can be seen from the example plots in Figures 2.2 and 2.3 for 1 1/4" copper line.

Ellis and Kruyer (8) have attempted to correlate the pressure gradient and the liquid velocity through an equivalent velocity defined as

$$V_{eq} = V_{an} - A\, V_c \tag{2.27}$$

where A is an arbitrary constant parameter and V_{an} is the velocity in the annulus. Consequently Reynolds number is

$$Re = \frac{(D-d)(V_{an} - A\, V_c)}{\nu} \tag{2.28}$$

TABLE 2.9

PRESSURE DROP MEASUREMENT VARIANCE

FOR 1 1/4" COPPER LINE

CARRYING STEEL CAPSULES

Run No.	k	σ	Range of PGC	Variance σ_*^2	95% Limits
408	.9400	1.031	.0 - .03	9.0×10^{-7}	± .002
418	.8895	1.125	.02 - .035	1.1×10^{-6}	± .002
428	.8390	1.25	.045 - .06	4.5×10^{-6}	± .004
436	.8390	1.5	.07 - .085	6.2×10^{-6}	± .005
442	.8895	2	.16 - .20	9×10^{-6}	± .006
448	.9400	3	.32 - .45	1.3×10^{-4}	± .023
450	.8895	3	.2 - .45	5.7×10^{-3}	± .15
454	.7916	3	.17 - .30	4.8×10^{-3}	± .14
456	.9400	5	.5 - 1.0	1.9×10^{-2}	± .28
458	.8895	5	.5 - 1.0	1.3×10^{-2}	± .23

A semi-empirical justification may be given here for this kind of equivalent velocity. Capsule flow in a pipe involves two relative velocities that contribute to the viscous drag:

a) annular velocity of the fluid relative to the pipe wall: V_{an}

b) annular velocity of the fluid relative to capsule wall: $V_{an} - V_c$, some kind of an average V_{an} is implied here.

The hydraulic radius is (D-d)/4. Assuming two fields are linear i.e., the two velocities can be linearly superimposed to determine the net viscous drag

$$V_{eq} = (1-A)V_{an} + A(V_{an}-V_c)$$

$$= V_{an} - A\,V_c$$

where A is simply a weighting factor which may or may not be a function of k, σ, D, ρ, ν.

It may be noted that besides making the assumption of linear superimposition, Ellis and Kruyer are assuming A to be an absolute constant independent of k, σ, ρ, etc. and that there is no form drag. The last assumption is not unreasonable in the light of our results of the preceeding section. The absence of terms containing V_b^2 in the capacity relations implies no significant form drag.

However, this and other modeling techniques can be usefully employed only when more reliable data under controlled conditions can be generated. In the meanwhile, we turn our attention to examining the capsule flow mechanism in somewhat greater detail in the next chapter.

3. A THEORETICAL MODEL FOR THE LAMINAR PIPE FLOW OF CAPSULES

3.1 Scope

The mechanism of capsule flow in a pipe is extremely complicated due to the large number of variables affecting the flow. What has become obvious now is that no simple mechanism can adequately explain the relationship among the variables. In spite of over a decade of effort in this area, no satisfactory solution is available for designing the capsule pipelines. Limited success, such as in Chapter 2, has been met in obtaining capacity correlations but the problem of predicting pressure drop in the capsule system remains largely unsolved. An examination of pressure drops suggests the presence of variables that have not been taken into account.

What is required is an examination of the physics of the capsule flow problem. A significant body of results are available to test any theoretical hypotheses. For example, it is known that the capsule normally travels at a slight angle to the pipe axis with nose-up position and that only a very small clearance (not usually observable) exists between the capsule and the pipe bottom, even for capsules with density nearly equal to that of the liquid. The effect of capsule density is quite pronounced on the pressure gradient but that of the length is negligible over the range of experimentation (length/diameter ratio more than 6). Other observations are noted in section 1.1.

3.2 A Preliminary Physical Model

One can visualize a capsule being conveyed with a velocity V_c by a liquid with a parabolic velocity profile. Secondary flows are generated from the requirements of continuity and are illustrated in Figure 3.1. The situation in Figure 3.1(b) is typical of conditions encountered in the range of practical velocities.

However, it may be noted that the forces due to these secondary flows act in opposite direction at the two ends and thus the net force upward or downward will be negligible, although there may be an important contribution to the torque balance on the capsule. There must then be other forces to support the excess weight of the capsule. The analogy with the slipper bearing is obvious and has long been recognized (5). In the slipper bearing, the slipper moving at a slight angle to the bearing with a wedge of liquid in between generates enough pressure in the liquid film to support its weight. In the capsule flow, the capsule surface could be visualized as a series of slippers of infinitesimal width moving at a slight angle to the pipe surface (of course both the clearance and the angle differ with each infinitesimal surface).

Thus the liquid flow field could be considered hopefully to be the linear superimposition of the two independent flows: (a) Couette flow due to the liquid being carried along the moving capsule, (b) the pressure flow of liquid flowing through the annulus formed between the stationary capsule and pipe surface.

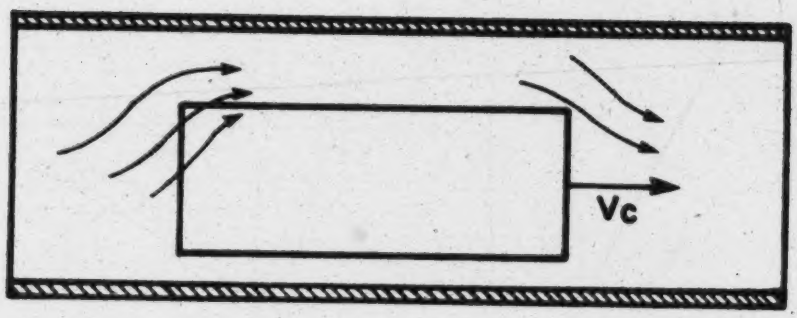

(a) Vc is small compared to liquid bulk velocity Vb.

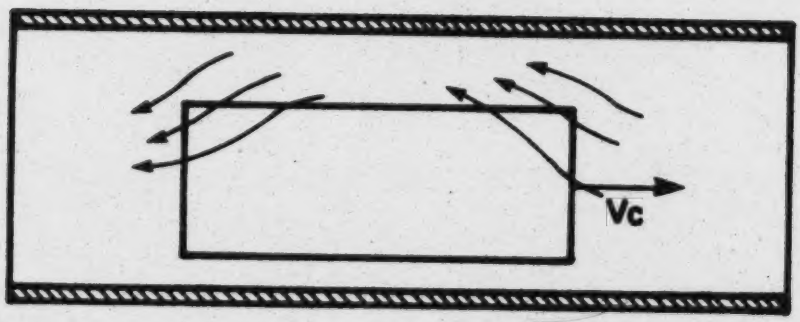

(b) Vc is of the order of Vb.

Figure 3.1 Secondary flows around the capsule.

3.3 Couette Flow

3.3.1 Plane Slipper Bearing

Prandtl (25) derived the motion of a parallel slipper on a guide by making the following simplifying assumptions (Figure 3.2).

(a) $p' = \frac{dp}{dx}$, the pressure gradient in the axial x direction is independent of y on account of the small clearance (h) between the slipper and the guide.

(b) Inertia terms are negligible.

(c) Conditions change slowly along the x-direction, i.e. $\frac{\partial^2 u}{\partial x^2}$ can be neglected compared to $\frac{\partial^2 u}{\partial y^2}$ where u is the liquid velocity.

(d) No leakage of fluid from the sides. This amounts to assuming negligible secondary flows in the capsule flow.

Consider a stationary slipper of unit width and a guide of length ℓ moving in the opposite direction with a velocity V_c (Figure 3.2). With the above assumptions, the equation of motion for the liquid in the interspace reduces to

$$\mu \frac{\partial^2 u}{\partial y^2} = \frac{dp}{dx} = p' \qquad (3.1)$$

where μ is the liquid viscosity.

Integrating and evaluating the constants from the boundary conditions

$$u = \frac{p'}{2\mu} (y^2 - h_x y) + \frac{V_c}{h_x} (h_x - y) \qquad (3.2)$$

h_x being the clearance at any point x .

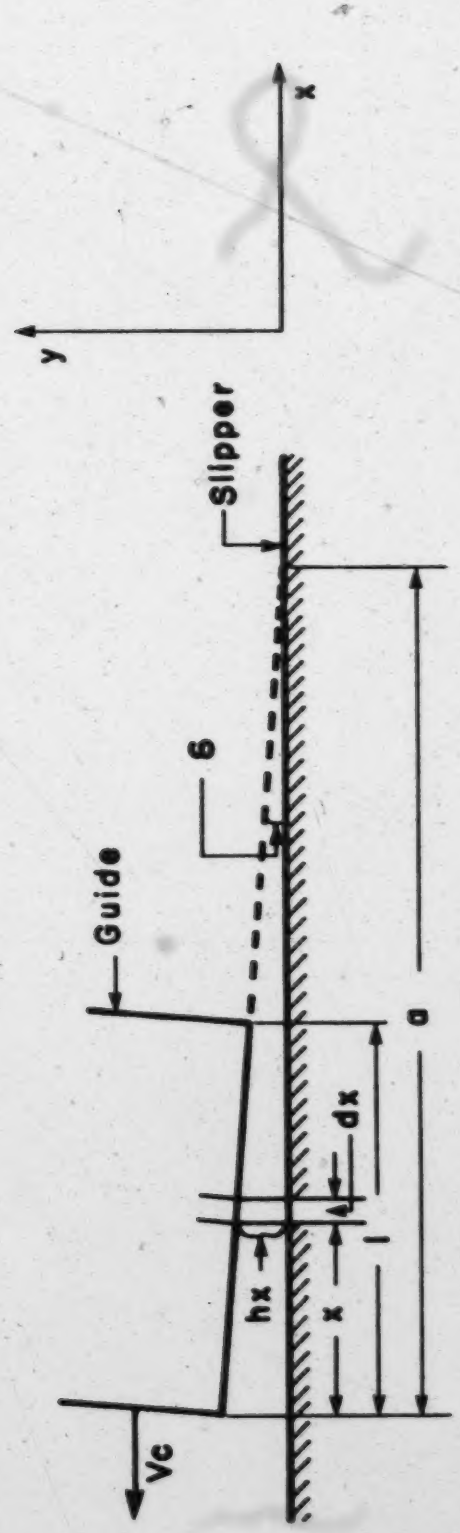

Figure 3.2 Guide moving in the opposite direction with stationary slipper.

$$Q = \int_0^{h_x} u \, d y$$

$$= \frac{V_c h_x}{2} - \frac{p' h_x^3}{12\mu} \qquad (3.3)$$

This gives

$$p' = 12 \mu \left(\frac{V_c}{2h_x^2} - \frac{Q}{h_x^3} \right) \qquad (3.4)$$

In case of the bearing, the pressure at $x = 0$ and $x = \ell$ must equal the ambient pressure p_o and thus the pressure must rise and go through maximum as x increases from 0 to ℓ. This has to be the case to balance the load carried by the slipper. The same holds true for the capsule flow ignoring for the present the pressure gradient PGC due to the pressure flow. From the geometry of Figure 3.2.

$$h_x = (a-x) \delta \qquad (3.5)$$

where δ is the wedge angle.

The excess pressure at any x is given by

$$p_x - p_o = \int_0^x p' \, dx \qquad (3.6)$$

Using (3.5) in (3.6)

$$p_x - p_o = \frac{6\mu x}{a\delta^2 (a-x)} \left(V_c - \frac{Q(2a-x)}{a \delta (a-x)} \right) \qquad (3.7)$$

but $p_x = p_o$, the ambient pressure at $x = \ell$, substituting

in (3.7) gives

$$Q = \frac{V_c \; a \; \delta(a-\ell)}{(2a-\ell)} \tag{3.8}$$

and

$$p_x - p_o = \frac{6\mu V_c \; x(\ell-x)}{h_x^2 \; (2a-\ell)} \tag{3.9}$$

Figure 3.3 gives an illustrative plot of pressure over the length of the guide as well as the form of the velocity profiles in the interspace.

Prandtl obtained simplified approximate expressions for the mean pressure and friction on the slipper by assuming parabolic pressure distribution. We will proceed further by using the expression in (3.9).

The total vertical force per unit width on the guide and the slipper is given by

$$w = \int_0^{\ell} (p_x - p_o) \, dx \tag{3.10}$$

Substituting for $(p_x - p_o)$ from (3.9), the above integral can be reduced to

$$w = \frac{6\mu V_c}{\delta^2 (2a-\ell)} \{(2a-\ell) \; \ln \left(\frac{a}{a-\ell}\right) - 2\ell) \tag{3.11}$$

If $a >> \ell$, $(\ell/a-\ell)$ is small, then

$$\ln \frac{a}{a-\ell} = \ln\left(1 + \frac{\ell}{a-\ell}\right)$$

$$\simeq \frac{\ell}{a-\ell} \tag{3.12}$$

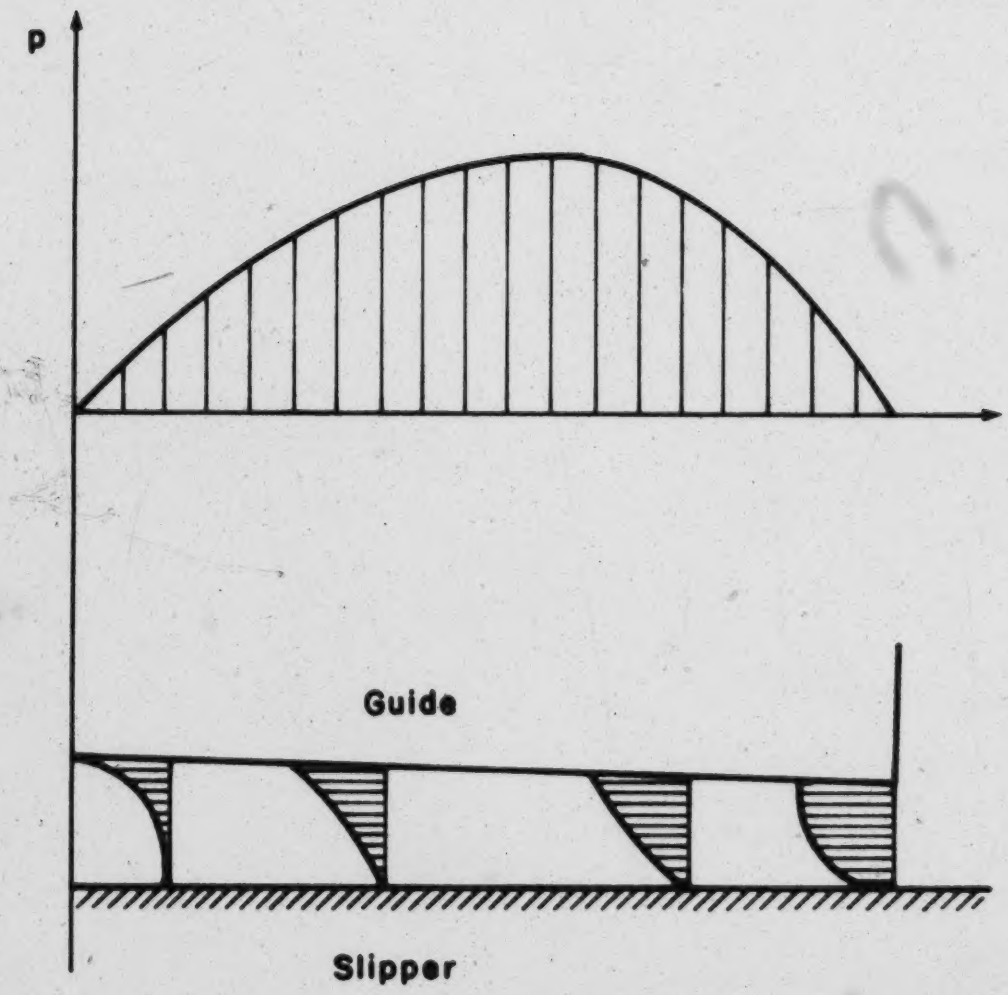

Figure 3.3 Pressure and velocity profiles for slipper bearing.

Substituting in (3.11)

$$w = \frac{6\mu V_c \ell^2}{\delta^2 (2a-\ell)(a-\ell)}$$

$$= \frac{3\ell^2 \mu V_c}{h_m h_\ell} \qquad (3.13)$$

where $h_m = h_{\ell/2}$, clearance at the midpoint.

Force of friction on the upper surface (capsule) will be positive and given by

$$\tau_c = -\mu \left(\frac{\partial u}{\partial y}\right)_{y = h_x}$$

$$= \mu \frac{V_c}{h_x} - p' \frac{h_x}{2} \qquad (3.14)$$

Substituting for p' from (3.4)

$$\tau_c = \mu \frac{V_c}{h_x} - 6\mu \left(\frac{V_c}{2h_x} - \frac{Q}{h_x^2}\right) \qquad (3.15)$$

and using (3.8) for Q

$$\tau_c = \frac{6\mu V_c \, a \, \delta \, (a-\ell)}{(2a-\ell) \, h_x^2} - \frac{2\mu V_c}{h_x} \qquad (3.16)$$

The total drag on a unit width of the guide (capsule) is

$$f_c = \int_0^\ell \tau_c \, dx \qquad (3.17)$$

Using the relation in (3.5) for h_x and solving the above integral

$$f_c = \frac{3\mu V_c \ell}{h_m} + \frac{\mu V_c (2a-\ell)}{h_m} \ln\left(\frac{a-\ell}{a}\right) \tag{3.18}$$

Again, if $a >> \ell$ (3.18) simplifies to

$$f_c = \frac{3\mu V_c \ell}{h_m} - \frac{2\mu V_c \ell}{h_o} \tag{3.19}$$

Since $h_m < h_o$, f_c will always be positive.

It may be interesting to note that Prandtl obtained $\mu V_c/h_m$ as an expression for the mean shear stress assuming a trapezoidal form for the shear stress distribution. Equation (3.19) also reduces to Prandtl's form if the assumption of $a >> \ell$ is carried to its logical conclusion, i.e. $h_m = h_o$. In general, (3.19) predicts somewhat higher drag.

The assumption $a >> \ell$ implies that the clearance varies only gradually along the length of the capsule or slipper bearing. This seems reasonable in the light of actual experimental observations of the capsule flow over wide range of liquid viscosities, capsule densities, diameter ratios and liquid flow rates. We shall also use this assumption at a subsequent stage of this analysis.

From (3.13), it is apparent that the vertical thrust due to the pressure distribution in the clearance is approximately inversely proportional to the square of the clearance. This implies that the bearing effect in the capsule mechanism is only significant over a small lower portion. Thus all the qualitative features of this flow

mechanism can be inferred from a parallel slipper bearing. Furthermore, since the flow in this small lower section of the capsule system will generally be laminar regardless of the nature of flow in the upper layers, these inferences hold for all flow regimes.

For example, the effect of roughness of both the capsule and pipe surfaces on the pressure drop in the capsule flow would be to cause a series of sudden bumping of the rear end of the capsule, i.e. where the clearance is least. This means h_ℓ will be increased at each bump. From relation (3.13), it is clear that to support the same excess weight either V_c should increase or the mean clearance should decrease. The former would require large accelerating forces from the liquid flow field to act on the capsule and consequently does not seem likely. Furthermore, V_c versus V_b plots for diverse capsule flow conditions have been found to be relatively smooth. Thus the mean clearance between the capsule and the pipe bottom must decrease resulting in increasing drag on the capsule surface and hence an increase in PGC (in equation (3.19) increased V_c also leads to similar results).

Theoretically, the two surfaces of capsule and pipe should never come in contact, for that would mean zero clearance which would generate very large pressures that cannot be balanced by the excess weight. This would be true if there were no secondary flows (side leakages), absolutely smooth surfaces, completely laminar flow in the entire annulus and also no end effects. To the extent the actual conditions differ from the ideal, the motion of the capsule would be characterized by random deviations from its most likely path with some deviations large enough to cause bumping of the two surfaces. The secondary flows, as long as they are uniform, cause the mean clearance to be consistently less than

that predicted by the no-leakage slipper bearing analysis. The roughness of the two surfaces, particularly for low viscosity liquids, aided by turbulent liquid eddies, may cause vertical and angular swings occasionally large enough to break the liquid film and result in dragging motion. In this sense, both the clearance and angle of capsule inclination may be regarded as random or more appropriately stochastic variables.

When a capsule is run repeatedly to and fro on a pipe surface without rotation (so that the same two surfaces face each other), in the light of the above discussion, it is presumed that the surfaces change with time both in the degree and in the type of roughness. Large protruding humps are gradually shaved or worn off and troughs filled with metal flow from adjoining high areas. On the other hand, very smooth surfaces might be roughened to some extent by the nonuniform wear and hammering effect of collisions.* One would also expect the tail end of the capsule to be worn off more than the nose end. It is logical to conclude that there is an equilibrium or ultimate roughness which is a function of the materials of the two surfaces and possibly a weak function of the capsule velocity. However, it may take different lengths of running times to achieve an ultimate roughness, say only a few hours for a capsule train with a fast moving low viscosity liquid carrier to an almost infinite time for a slow moving high viscosity liquid.

The effect of the surface roughness will be negligible for viscous laminar flow due to the larger clearance, and the absence of turbulent disturbances which could cause a wave-like motion of the capsule.

---

*This effect was actually observed at the Research Council of Alberta by J. Kruyer.

For low viscosity turbulent flows, end effects and turbulent eddies both combine to cause wide fluctuations in the pressure drop. Furthermore, since the mean thickness and angle of inclination of the capsule are functions of the surface roughness, the pressure gradient would also be a function of the surface roughness.

Another interesting empirical observation is regarding the effect of mounting collars on the front half of the capsule. In the experiments at the Research Council of Alberta, such collars have been observed to drastically reduce the pressure drop -- by as much as 80% (10). The slipper bearing model readily explains the observed phenomenon. A collar in the front half of the capsule would result in a greater angle both due to the physical presence of the collar and the increased secondary flows at the nose end because of the additional liquid being swept forward from the slow moving liquid layers at the bottom. The increased angle of inclination has to be accompanied by an increase in the mean clearance to support a given weight of the capsule. The pressure gradient, being approximately inversely proportional to the mean clearance, is reduced as the mean clearance increases with the incorporation of the collar.

Before further conclusions can be drawn from this model, we need to extend this model to account for the circular shape of the capsule and also to include the pressure flow.

3.3.2 Capsule Couette Flow Model

Consider now a capsule being pulled by a force F with a velocity V_c in a pipe full of liquid where the only flow is due to the motion of the capsule. Any two facing surfaces on the capsule and pipe of infinitesimal width along the length may be considered as a slipper bearing of given "a" and "δ". Let θ be the angle that the infinitesimal

slipper bearing makes with the vertical axis. The points A and B are the centres of pipe and capsule respectively (Figure 3.4). For our analysis we shall consider the point O , the midpoint of these two centres, as the approximate centre for the annulus. If ε is the eccentricity of the two centres, r and R the radii of the capsule and the pipe respectively, it can be seen that

$$OC = r + \frac{\varepsilon}{2} \cos \theta \tag{3.20}$$

$$OP = R - \frac{\varepsilon}{2} \cos \theta \tag{3.21}$$

The clearance at the mid point

$$\begin{aligned} PC = h(\theta) &= OP - OC \\ &= R - r - \varepsilon \cos \theta \end{aligned} \tag{3.22}$$

Now, the total drag F_c on the capsule is obtained simply by integrating the drag forces on a series of infinitesimal slippers.

$$F_c = \int_0^{2\pi} f_c (r)\, d\theta \tag{3.23}$$

Using relation (3.19) for f_c

$$F_c = 2 \int_0^{\pi} \left(\frac{3\mu V_c \ell}{h_m} - \frac{2\mu V_c \ell}{h_o} \right) r d\theta \tag{3.24}$$

Using relation (3.22) we show in Appendix A that

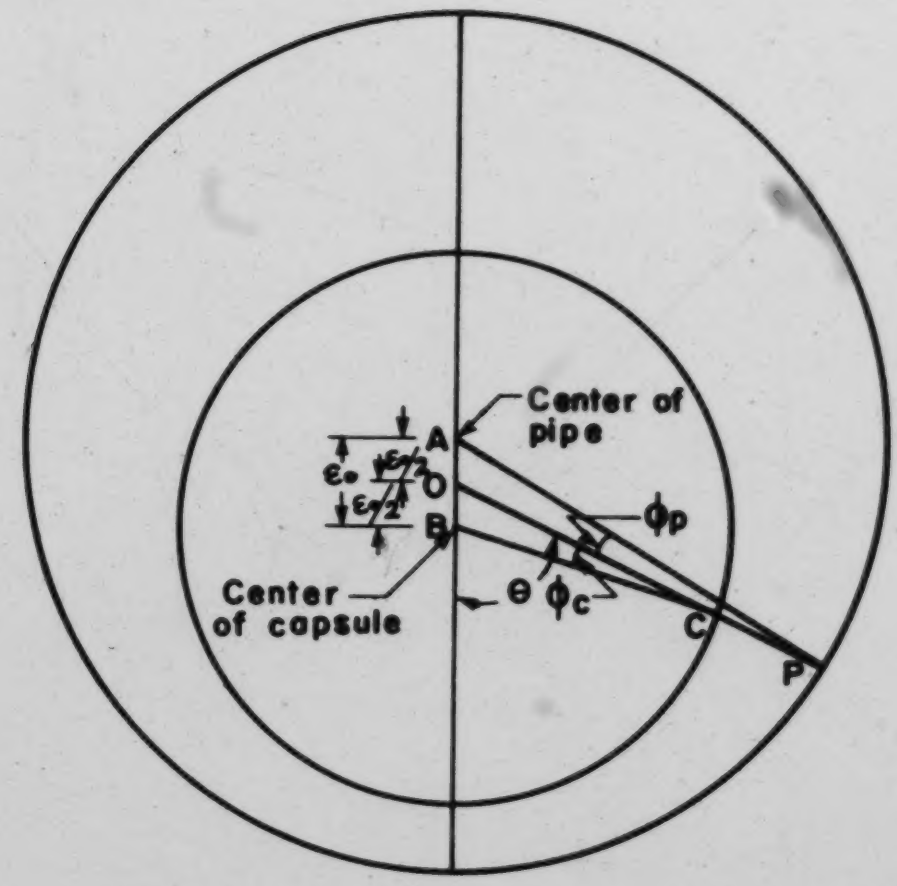

Figure 3.4 Endview of capsule and pipe.

$$F_c = \frac{2\pi\mu V_c \ell r}{(R-r)} \left[\frac{3}{\{1 - \frac{\varepsilon_m^2}{(R-r)^2}\}^{\frac{1}{2}}} - \frac{2}{\{1 - \frac{\varepsilon_o^2}{(R-r)^2}\}^{\frac{1}{2}}} \right] \qquad (3.25)$$

The capsule flow parameters a and δ (or ε_m and ε_o) are not free to take any values. They are constrained by the vertical force balance and torque balance (horizontal force balance determines V_c and PGC relationship). The net vertical component of the pressure force is

$$W = \int_0^{2\pi} w \cos\theta \, (r) \, d\theta \qquad (3.26)$$

Using relations (3.13) and (3.22) it is shown in Appendix B that

$$W = \frac{6\pi\mu\ell^2 V_c r}{\varepsilon_\ell (R-r)} \left[\frac{1}{\left[1 - \frac{(\varepsilon_m + \varepsilon_\ell)^2}{4(R-r)^2}\right]^{3/2}} - \frac{1}{\left[1 - \frac{\varepsilon_m^2}{(R-r)^2}\right]^{1/2}} \right] \qquad (3.27)$$

The pressure distribution, somewhat like that shown in Figure 3.3 , generates a torque in the vertical plane. The flow is symmetric in the cross direction and only the force components in the vertical direction need be considered.

With reference to Figure 3.4, the vertical component of force on an element (dx) (r dθ) at C is

$$d^2W = (p_x - p_o) \{dx(r\, d\theta)\} \cos\theta$$

$$= \frac{6\mu V_c \, x(\ell - x)}{h_x^2 \, (2a - \ell)} \, r \cos\theta \, dx \, d\theta \qquad (3.28)$$

The torque about A (Figure 3.2) is

$$T_v = \int_0^{2\pi} \int_0^{\ell} \frac{6\mu V_c \, x^2 (\ell - x)}{h_x^2 \, (2a-\ell)} \, r \cos\theta \, dx \, d\theta \qquad (3.29)$$

Again, using the relations (3.5) and (3.22) and assuming that the clearance is small compared to r and R, we show in Appendix C that

$$T_v = - \frac{6 \pi \mu V_c \, \ell^3 \, r \, \varepsilon_\ell}{(R-r)^3 \left[1 - \frac{\varepsilon_\ell^2}{(R-r)}\right]^{3/2}} \qquad (3.30)$$

Finally, we calculate the total Couette flow Q_c of the liquid due to the capsule motion, the liquid flow per unit width of slipper bearing being given by (3.8). For an infinitesimal strip at P (Figure 3.4), the width for flow is approximately $(\frac{OC + OP}{2})d\theta$.

$$dQ_c = \frac{V_c \, a \, \delta \, (a-\ell)}{(2a-\ell)} \, \frac{(OC + OP)}{2} \, d\theta \qquad (3.31)$$

Using relations (3.5), (3.20), (3.21), and (3.22)

$$dQ_c = \frac{V_c \, h_o \, h_\ell}{2 \, h_m} \, \frac{(r + \varepsilon/2 \cos\theta + R - \varepsilon/2 \cos\theta)}{2} \, d\theta$$

$$= \frac{V_c (R + r)}{4} \, \frac{(R-r-\varepsilon_o \cos\theta)(R-r-\varepsilon_\ell \cos\theta)}{(R-r-\varepsilon_m \cos\theta)} \, d\theta \qquad (3.32)$$

$$Q_c = \int_0^{\pi} \frac{V_c(R+r)}{2} \frac{(R-r-\varepsilon_o \cos\theta)(R-r-\varepsilon_\ell \cos\theta)}{(R-r-\varepsilon_m \cos\theta)} d\theta$$

$$= \frac{V_c(R-r)}{2} \int_0^{\pi} \left(-\frac{\varepsilon_o \varepsilon_\ell}{\varepsilon_m} \cos\theta + \frac{(R-r)}{\varepsilon_m} (\varepsilon_o + \varepsilon_\ell - \frac{\varepsilon_o \varepsilon_\ell}{\varepsilon_m}) \right.$$

$$\left. + \frac{(R-r)^2}{\varepsilon_m} \frac{(\varepsilon_m - \varepsilon_o - \varepsilon_\ell + \frac{\varepsilon_o \varepsilon_\ell}{\varepsilon_m})}{(R - r - \varepsilon_m \cos\theta)} \right) d\theta$$

$$= \frac{V_c(R+r)}{2} \left(+ \frac{\varepsilon_o \varepsilon_\ell}{\varepsilon_m} \sin\theta \Big|_0^{\pi} + \frac{\pi(R-r)}{\varepsilon_m} (\varepsilon_o + \varepsilon_\ell - \frac{\varepsilon_o \varepsilon_\ell}{\varepsilon_m}) \right.$$

$$\left. + \frac{(R-r)(\varepsilon_m - \varepsilon_o - \varepsilon_\ell + \frac{\varepsilon_o \varepsilon_\ell}{\varepsilon_m})}{\varepsilon_m} \int_0^{\pi} \frac{d\theta}{(1 - \frac{\varepsilon_m \cos\theta}{(R-r)})} \right)$$

$$= \frac{\pi(R^2 - r^2)V_c}{2\varepsilon_m} (\varepsilon_m)$$

$$= \frac{\pi(R^2 - r^2) V_c}{2} \qquad (3.33)$$

It may be noted that (3.33) also gives the flow for concentric capsule flow with a perfectly linear velocity profile in the annulus.

3.4 Pressure Flow

Now consider a stationary capsule with liquid flowing through the annulus with an imposed pressure gradient PGC . We shall confine

our attention to the case where the flow in the annulus is laminar. Neglecting [illegible] effects and secondary flows and for the steady state conditions,

$$\frac{\partial}{\partial \psi}\left(\psi \frac{\partial u}{\partial \psi}\right) = -\frac{1}{\mu}(PGC)\,\psi \qquad (3.34)$$

With reference to Figure 3.4, u is the velocity at any angle θ and distance ψ from 0.

Integrating twice

$$\psi \frac{\partial u}{\partial \psi} = -\frac{\psi^2}{2\mu}(PGC) + C_1 \qquad (3.35a)$$

$$u = -\frac{(PGC)}{4\mu}\psi^2 + C_1 \ell_n \psi + C_2 \qquad (3.35b)$$

Using the end conditions $u = 0$ at $\psi = r + \frac{\epsilon}{2}\cos\theta$ and also $u = 0$ at $\psi = R - \frac{\epsilon}{2}\cos\theta$ to evaluate C_1 and C_2, equation (3.35b) reduces to

$$u = \frac{PGC}{4\mu}\left[-\psi^3 + \frac{(r_1^2 - r_2^2)}{\ell n \frac{r_1}{r_2}} \ell n \psi + \frac{r_2^2 \ell n\, r_1 - r_1^2 \ell n\, r_2}{\ell n \frac{r_1}{r_2}}\right] \qquad (3.36)$$

where $r_1 = R - \frac{\epsilon_m}{2}\cos\theta$ (3.37a)

and $r_2 = r + \frac{\epsilon_m}{2}\cos\theta$ (3.37b)

Again we have used ϵ_m for ϵ and consider it independent of x.

The total pressure flow in the annulus is given by

$$Q_p = \int_0^{2\pi} \int_{r_2}^{r_1} u \, (\psi \, d\theta) \, d\psi \tag{3.38}$$

We show in Appendix D that approximately

$$Q_p = \frac{5\pi R^4}{32\mu} (PGC) \, (1-k^2)(1-k)^2 \tag{3.39}$$

where $k = r/R$.

The results in (3.39) may be compared with those of Tiedt (26).

$$f = - \frac{(R-r)}{\rho \bar{u}^2} (PGC) \tag{3.40a}$$

where ρ is the liquid density and $\bar{u}$ is the average annulus velocity given by

$$\bar{u} = Q_p / \pi R^2 (1-k^2) \tag{3.40b}$$

The Reynolds Number is defined as

$$R_e = \frac{(D-d) \, \bar{u}}{\upsilon} \tag{3.40c}$$

This gives

$$f \, R_e = \frac{2\pi R^4 (PGC)}{\mu \, Q_p} (1-k^2)(1-k)^2 \tag{3.40d}$$

Substituting for Q_p (3.39) gives

$$f R_e = \frac{64}{5}$$

$$= 12.8 \qquad (3.40e)$$

The agreement of (3.40e) with the results obtained by Tiedt is not as good as might have been hoped for. Nevertheless, it is good enough for our purpose considering the approximations involved. According to Tiedt, for zero bottom clearance and k = 1/2, the value for f Re is 10.3 and it approaches 9.6 as k approaches unity.

The shear force on the capsule surface due to pressure flow is

$$\tau_p = - \mu \left(\frac{\partial u}{\partial \psi}\right)_{\psi=r_2} \qquad (3.41)$$

From (3.36)

$$\left(\frac{\partial u}{\partial \psi}\right)_{\psi=r_2} = \frac{PGC}{4\mu r_2} \left[- 2r_2^2 + \frac{(r_1^2 - r_2^2)}{\ln \frac{r_1}{r_2}} \right] \qquad (3.42)$$

Therefore

$$\tau_p = - \frac{PGC}{4\mu r_2} \left[- 2r_2 + \frac{(r_1^2 - r_2^2)}{\ln \frac{r_1}{r_2}} \right] \qquad (3.43)$$

From relation (D-5) Appendix D

$$\left(\frac{1}{\ell n \frac{r_1}{r_2}}\right) \approx \frac{r_2}{r_1 - r_2} + \frac{1}{2}$$

Consequently

$$\tau_p \approx - \frac{PGC}{4r_2} \left(- \frac{3}{2} r_2^2 + r_1 r_2 + \frac{1}{2} r_1^2 \right)$$

$$= - \frac{PGC}{4r_2} \left(\frac{1}{2} (r_1 + r_2)^2 - 2r_2^2 \right) \qquad (3.44)$$

The total force on the surface is

$$F_p = \int_0^{2\pi} \tau_p \, \ell \, r_2 \, d\theta$$

$$= - \frac{(PGC)\ell}{2} \int_0^{\pi} \left(\frac{1}{2} (r_1 + r_2)^2 - 2r_2^2 \right) d\theta$$

$$= - \frac{(PGC)\ell}{2} \int_0^{\pi} \left(\frac{1}{2} (R + r)^2 - 2r^2 - 2r\epsilon_m \cos\theta - \frac{1}{2}\epsilon_m^2 \cos^2\theta \right) d\theta$$

$$= - \frac{(PGC)\ell}{2} \left(\frac{\pi}{2} (R + r)^2 - 2\pi r^2 - \frac{\pi}{4}\epsilon_m^2 \right)$$

For small bottom clearance ($\epsilon_m \approx (R-r)$), the above reduces to

$$F_p = - \frac{\pi (PGC) \ell R^2}{8} (1-k)(1+7k) \qquad (3.45)$$

The moment in the vertical plane about D (Figure 3.5) caused by the horizontal shear forces on the surface due to both the Couette flow and the pressure flow is

$$dT_h = (f_c\, r\, d\theta + \tau_p\, \ell\, r\, d\theta)\, r(1 - \cos\theta) \qquad (3.46)$$

Using relations (3.19) and (3.44), it is shown in Appendix E that

$$T_h = 2\pi\mu V_c \ell r^2 \left[\frac{3}{\varepsilon_m} - \frac{2}{\varepsilon_o} - \frac{3(R - r - \varepsilon_m)}{\varepsilon_m (R-r) \left(1 - \frac{\varepsilon_m^2}{(R-r)^2}\right)^{\frac{1}{2}}} + \frac{2(R - r - \varepsilon_o)}{\varepsilon_o (R-r) \left(1 - \frac{\varepsilon_o^2}{(R-r)^2}\right)^{\frac{1}{2}}} \right]$$

$$+ \frac{\pi (PGC) \ell r^2}{8} \left[\frac{2(\varepsilon_m + R + r)(R + r)}{\varepsilon_m} + 2\left(R - r - \frac{\varepsilon_m}{2}\right) - \frac{(R + r)^2 (\varepsilon_m + 2r)}{\varepsilon_m r \left(1 + \frac{\varepsilon_m^2}{4r^2}\right)^{\frac{1}{2}}} \right] \qquad (3.47)$$

3.5 Total Flow

We now superimpose the Couette and the pressure flows. We assume the two flow fields are linear, i.e. their effects are additive. From the requirements of continuity

Total flow = Couette flow + Pressure flow + Capsule flow

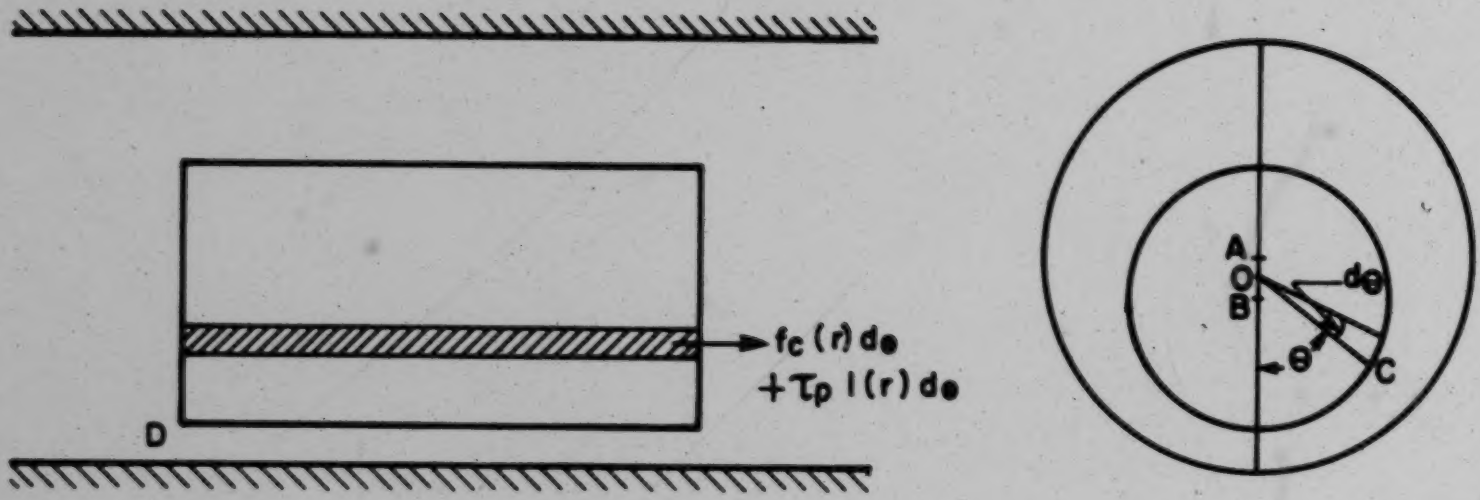

Figure 3.5 An infinitesimal surface on the capsule.

or

$$\pi R^2 V_b = Q_c + Q_p + \pi r^2 V_c \tag{3.48}$$

where V_b is the bulk or the average velocity in the capsule flow system. Substituting for Q_c and Q_p from (3.33) and (3.39)

$$V_b = \frac{5R^2}{32\mu} (PGC) (1-k^2)(1-k)^2 + \frac{1}{2} (1+k^2) V_c \tag{3.49}$$

The forces acting on the capsule must balance. For example, if secondary flows are neglected the excess weight of the capsule

= Vertical component of the excess pressure due to Couette flow.

or

$$\pi r^2 (\sigma - \rho) g \ell = W \tag{3.50}$$

Substituting for W from (3.27)

$$r(\sigma - \delta)g = \frac{6\mu \ell V_c}{\epsilon_\ell (R-r)} \left(\frac{1}{\left(1 - \frac{(\epsilon_m+\epsilon_\ell)^2}{4(R-r)^2}\right)^{3/2}} - \frac{1}{\left(1 - \frac{\epsilon_m^2}{(R-r)^2}\right)^{1/2}} \right) \tag{3.51}$$

When the clearance is small, so that $\epsilon_m = \epsilon_\ell = (R-r)$, the second term in the parentheses is much smaller than the first

$$r(\sigma - \rho)\, g = \frac{6\mu\, \ell\, V_c}{\varepsilon_\ell (R-r)} \left(\frac{1}{\left(1 - \frac{\varepsilon_m\, \varepsilon_\ell}{4(R-r)^2}\right)^{3/2}} \right)$$

or

$$\varepsilon_\ell^{2/3} \left(1 - \frac{(\varepsilon_m + \varepsilon_\ell)^2}{4(R-r)^2}\right) = \left(\frac{6\mu\, \ell\, V_c}{r(\sigma-\rho)\, g(R-r)} \right)^{2/3} \qquad (3.52)$$

Similarly, the forces in x-direction must balance, i.e.

Pressure force + viscous drag due to Couette flow + viscous drag due to pressure flow = 0

or

$$-\pi r^2\, \ell (PGC) + \frac{2\pi\mu V_c\, \ell r}{(R-r)} \left(\frac{3}{\left(1 - \frac{\varepsilon_m^{\,2}}{(R-r)^2}\right)^{1/2}} - \frac{2}{\left(1 - \frac{\varepsilon_o^{\,2}}{(R-r)^2}\right)^{1/2}} \right)$$

$$- \frac{\pi \ell\, (PGC)\, R^2}{8} (1-k)(1+7k) = 0 \qquad (3.53)$$

Moment about A due to Couette pressure forces + Moment due to excess weight + Moment due to all viscous forces = 0

or

$$T_v + \pi r^2 g(\sigma-\rho)\, \ell\, \frac{\ell}{2} + T_h = 0$$

i.e.

$$-\frac{6\pi\mu V_c \ell^3 r\, \varepsilon_\ell}{(R-r)^3\left(1-\frac{\varepsilon_\ell^2}{(R-r)^2}\right)^{3/2}} + \frac{1}{2}\pi r^2 g(\sigma-\rho)\,\ell^2$$

$$+ 2\pi\mu V_c \ell r^2 \left[\frac{3}{\varepsilon_m} - \frac{2}{\varepsilon_o} - \frac{3(R-r-\varepsilon_m)}{(R-r)\varepsilon_m\left(1-\frac{\varepsilon_m^2}{(R-r)^2}\right)^{\frac{1}{2}}} \right.$$

$$\left. + \frac{2(R-r-\varepsilon_o)}{(R-r)\varepsilon_o\left(1-\frac{\varepsilon_o}{(R-r)^2}\right)^{\frac{1}{2}}} \right]$$

$$- \frac{\pi\,(PGC)\ell r^2(R+r)}{8\,\varepsilon_m} \left[\frac{(R+r)(\varepsilon_m+2r)}{\left(r^2+\frac{\varepsilon_m^2}{4}\right)^{\frac{1}{2}}} - 2(R+r+\varepsilon_m) \right.$$

$$\left. - \frac{2\left(r-\frac{\varepsilon_m}{4}\right)\varepsilon_m}{(R+r)} \right] = 0 \qquad (3.54)$$

Also

$$\varepsilon_m = \frac{\varepsilon_\ell+\varepsilon_o}{2} \qquad (3.55)$$

We now have five equations (3.49),(3.52), (3.53), (3.54), (3.55) and five unknowns viz. V_c , PGC , ε_m , ε_ℓ , and ε_o .

When the clearance and the angle δ are small, it can be shown (Appendix F) that

$$PGC = \frac{8 \mu k V_c^{2/3}}{R(1 + 6k + k^2)} \left[\frac{4 k g (\sigma-\rho)}{3 \mu \ell (1-k)} \right]^{1/3} \qquad (3.56)$$

and

$$V_b = \left[\frac{5 k (1-k)^2 (1-k^2)}{4(1 + 6k + k^2)} \right] \left[\frac{4 k g (\sigma-\rho)}{3 \mu \ell (1-k)} \right]^{1/3} R V_c^{2/3} + \frac{1}{2} (1+k^2) V_c \qquad (3.57)$$

and for a high viscosity liquid

$$PGC = \frac{16 \mu k V_b^{2/3}}{R(1+k^2)(1 + 6k + k^2)} \left[\frac{2k(1+k) g (\sigma-\rho)}{3 \mu \ell (1-k)} \right]^{1/3} \qquad (3.58)$$

It may be noted that torque balance was not used to arrive at the above results; thus the significant effect of secondary flows on the torque did not enter our results.

3.6 Physical Contact of Surfaces

Frequent bumping of the capsule into the pipe surface and actual dragging at one end would cause an additional drag force and an upward reaction force on the capsule. The upward reaction force F_u may be considered as

$$F_u = \left(\phi \left[\frac{c_m}{(R-r)} \right] \right) \pi r^2 g \ell (\sigma-\rho) \qquad (3.59)$$

and the horizontal drag F_h, positive in the x-direction, is

$$F_h = \eta \left[\phi\left(\frac{\epsilon_m}{(R-r)}\right)\right] \pi r^2 \ell (\sigma-\rho) \qquad (3.60)$$

where η is the coefficient of wet friction (i.e. two surfaces are wetted by the carrier liquid).

Thus (3.50) becomes

$$r(\sigma-\rho)g\left[1+\phi\left(\frac{\epsilon_m}{(R-r)}\right)\right] = \frac{6\mu\ell V_c}{\epsilon_\ell (R-r)}\left[\frac{1}{\left(1-\frac{(\epsilon_m+\epsilon_\ell)^2}{4(R-r)^2}\right)^{3/2}} - \frac{1}{\left(1-\frac{\epsilon_m^2}{(R-r)^2}\right)^{1/2}}\right] \qquad (3.61)$$

Proceeding as before, (3.61) reduces to

$$\left(1-\frac{\epsilon_m^2}{(R-r)^2}\right) = \left[\frac{6\mu\ell V_c}{r(R-r)^2(\sigma-\ell)g\left[1+\phi\left(\frac{\epsilon_m}{(R-r)}\right)\right]}\right]^{2/3} \qquad (3.62)$$

Similarly (3.51) results in

$$PGC = \frac{16\mu V_c k}{R^2(1-k)(1+6k+k^2)}\left[\frac{1}{\left(1-\frac{\epsilon_m^2}{R^2(1-k)^2}\right)^{1/2}} + k^2 g\eta\phi\left(\frac{\epsilon_m}{(R-r)}\right)\right] \qquad (3.63)$$

Substituting from (3.62)

$$PGC = \frac{8\,\mu\,k\,V_c^{2/3}}{R(1+6k+k^2)} \left[\frac{4k(\sigma-\rho)\,g \left[1+\phi\left(\frac{\epsilon_m}{(R-r)}\right)\right]}{3(1-k)\,\mu\,\ell} \right]^{1/3} + k^2\,g\,\eta\,\phi\left(\frac{\epsilon_m}{(R-r)}\right) \qquad (3.64)$$

Substituting PGC from (3.64) in (3.49)

$$V_b = \frac{5R(1-k^2)\,(1-k)^2\,k}{4(1+6k+k^2)} \left[\frac{4k(\sigma-\rho)\,g \left[1+\phi\left(\frac{\epsilon_m}{(R-r)}\right)\right]}{3(1-k)\,\mu\,\ell} \right]^{1/3} V_c^{2/3} + \frac{5R^2(1-k^2)(1-k)^2\,k^2 g\,\eta}{32\,\mu}\,\phi\left(\frac{\epsilon_m}{(R-r)}\right) + \frac{1}{2}\,(1+k^2)\,V_c \qquad (3.65)$$

From (3.59), $\phi\left(\frac{\epsilon_m}{(R-r)}\right)$ may be interpreted as the fraction of the excess weight supported by the surface reaction or that supported by secondary flows. Thus ϕ may be an empirical term that incorporates the effect of all simplifying assumptions in our model.

When ϕ is small compared to unity, i.e.

$$1 + \phi\left(\frac{\epsilon_m}{(R-r)}\right) \simeq 1 \qquad (3.66)$$

(3.64) reduces to

$$PGC = \frac{8\,\mu\,k\,V_c^{2/3}}{R(1+6k+k^2)} \left(\frac{4k(\sigma-\rho)g}{3(1-k)\mu\,\ell}\right)^{1/3} + k^2\,g\,\eta\,\phi\left(\frac{\epsilon_m}{(R-r)}\right) \qquad (3.67)$$

and (3.65) now gives

$$V_b = \frac{5R(1-k^2)(1-k)^2k}{4(1+6k+k^2)}\left(\frac{4k(\sigma-\rho)g}{3(1-k)\mu\ell}\right)^{1/3} V_c^{2/3}$$

$$+ \frac{5R^2(1-k^2)(1-k)^2\,k^2\,g\,\eta}{32\,\mu}\,\phi\left(\frac{\epsilon_m}{(R-r)}\right) + \frac{1}{2}(1+k^2)\,V_c \qquad (3.68)$$

3.7 Threshold Velocity

Threshold velocity is the liquid bulk velocity which just sets the capsule moving. Since the mechanism of flow is the same, equation (3.65) should yield the threshold velocity $V_{b,t}$ when $V_c = 0$ except that now η would have to be replaced by η_s, the coefficient of static wet friction. Thus

$$V_{b,t} = \frac{5R^2(1-k^2)(1-k)^2\,k^2\,g\,\eta_s}{32\,\mu}\,\phi\left(\frac{\epsilon_m}{(R-r)}\right) \qquad (3.69)$$

3.8 Model Validation

In view of the assumptions made in the derivation, we would not expect the model to be able to predict quantitatively the true relationship between the different physical variables. Hopefully, the model would predict the right trends and suggest the form of some of the relationships.

We have selected a typical run, No. 64, from the Research Council of Alberta data, which involved the transport of steel capsules in oil in a 1/2" diameter copper line. Figures 3.6 and 3.7 give comparisons of the observed and predicted relationships between V_b and PGC (equations (3.56)

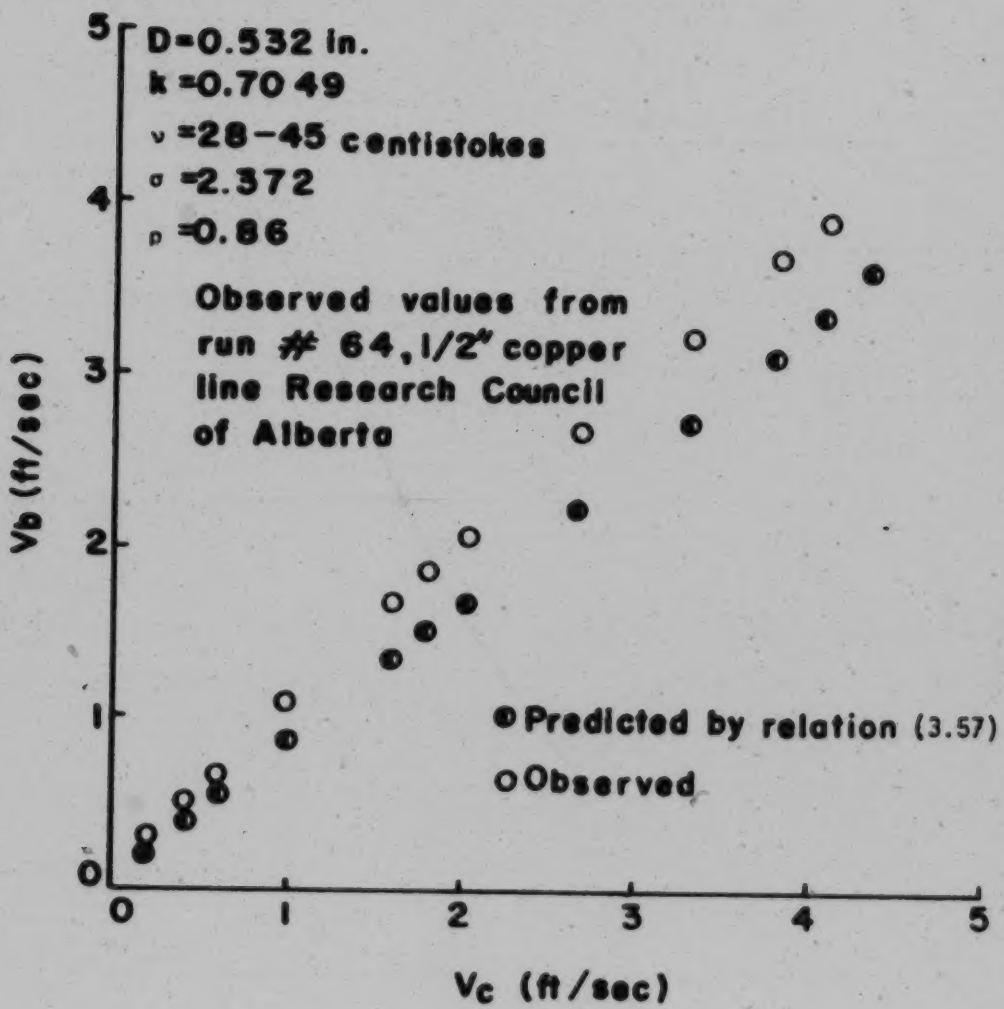

Figure 3.6 V_b versus V_c plots for 1/2" copper line carrying steel capsules in oil.

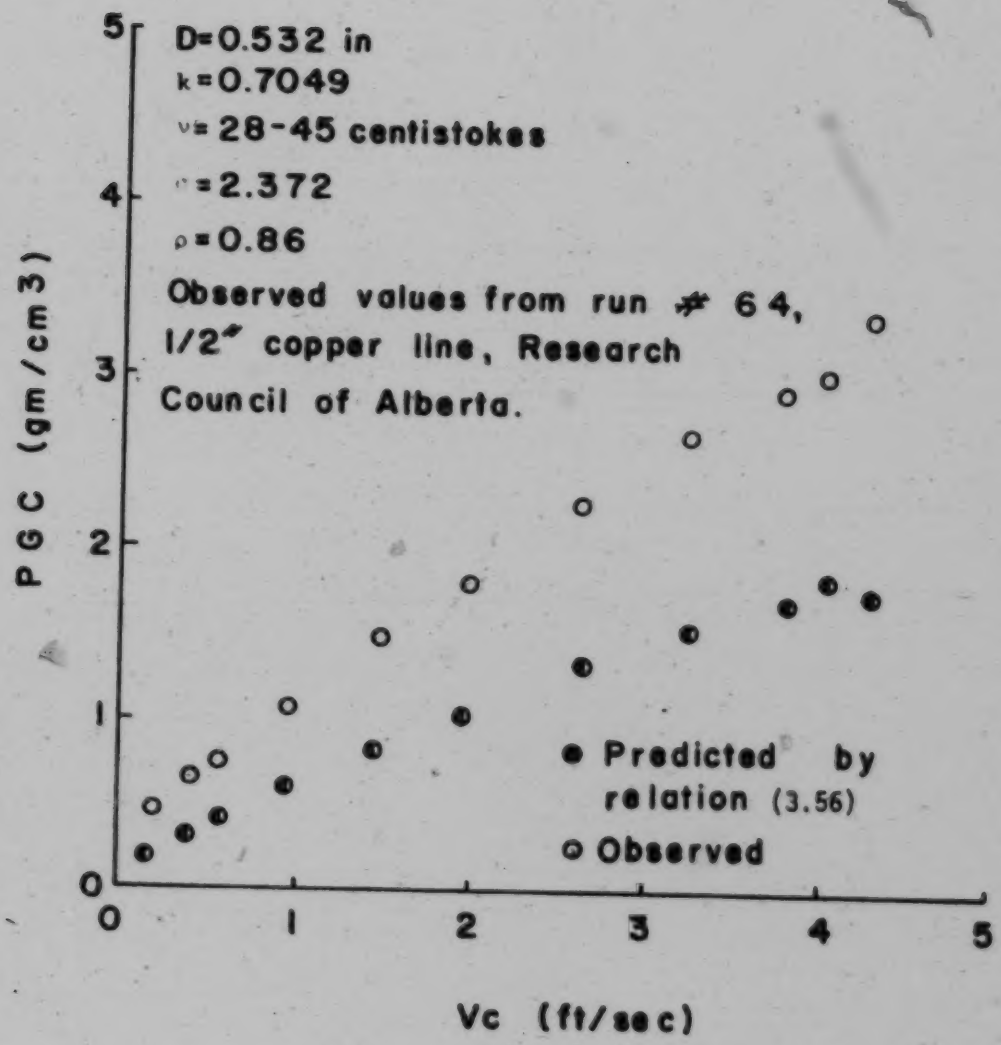

Figure 3.7 PGC versus Vc plots for 1/2" copper line carrying steel capsules in oil.

and (3.57)) on the one hand and V_b on the other.

As expected, both the predicted V_b and PGC for a given V_c are lower than the corresponding observed values. On examining the key assumptions used in deriving equations (3.56) and (3.57) namely, laminar flow, sufficiently small bottom clearance compared to R-r , and the absence of any secondary flows, we feel that the least warranted assumption is the last one. The bottom clearance would be significantly decreased by the presence of secondary flows (analogous to the side leakage in the slipper bearing, reference 25) causing greater drag on the capsule. Consequently in actual pipeline capsule flow with secondary flows, a liquid bulk velocity higher than that predicted by the model would be required to achieve a given capsule velocity. Also the pressure gradient observed should be higher than that predicted.

In addition, surface roughness and capsule fluctuations would cause the capsule to be in physical contact with the pipe bottom for a certain fraction of the time. This would result in additional drag on the capsule and thus compound the effect of secondary flows.

Comparing the results of this model (V_b versus V_c) with the empirical relations obtained in Chapter 2 from the data of the Research Council of Alberta, the two model forms look somewhat different. The empirical results for 1/2" copper line in laminar flow indicate V_b is proportional to V_c whereas equation (3.57) includes two terms, one proportional to V_c and the other proportional to $V_c^{2/3}$, and the latter term although smaller than the first is significant. However, it was found that the prediction of equation (3.57) was quite close to the straight line relationship (see Figure 3.6 as an example) found empirically. Pressure drop data could not be relied upon for a meaningful comparison.

The utility of this model can be further enhanced by an empirical modification. Incorporation of one free parameter each in relations (3.56) and (3.57) results in much better agreement with the experimental results. The predictions for the modified relations

$$PGC = b_1 \left[\frac{8 \mu k V_c^{2/3}}{R(1+6k+k^2)}\right] \left[\frac{4k g (\sigma-\rho)}{\mu \ell (1-k)}\right]^{1/3} \qquad (3.70)$$

and

$$V_b = b_2 \left[\frac{5k(1-k)^2(1-k^2)}{4(1+6k+k^2)}\right] \left[\frac{4k g (\sigma-\rho)}{3 \mu \ell (1-k)}\right]^{1/3} R V_c^{2/3} + \frac{1}{2}(1+k^2) V_c \qquad (3.71)$$

are shown in Figures (3.8) and (3.9). The parameters b_1 and b_2 are estimated from the experimental data themselves giving the following least square estimates

$b_1 = 1.714 \pm 0.0443$ (95% confidence limits)

Standard deviation of fit for model (3.70)

= 0.0983 or approximately 5% of the average prediction.

$b_2 = 187.1 \pm 14.08$

Standard deviation of fit for model (3.71)

= 0.087 or approximately 3% of the average prediction.

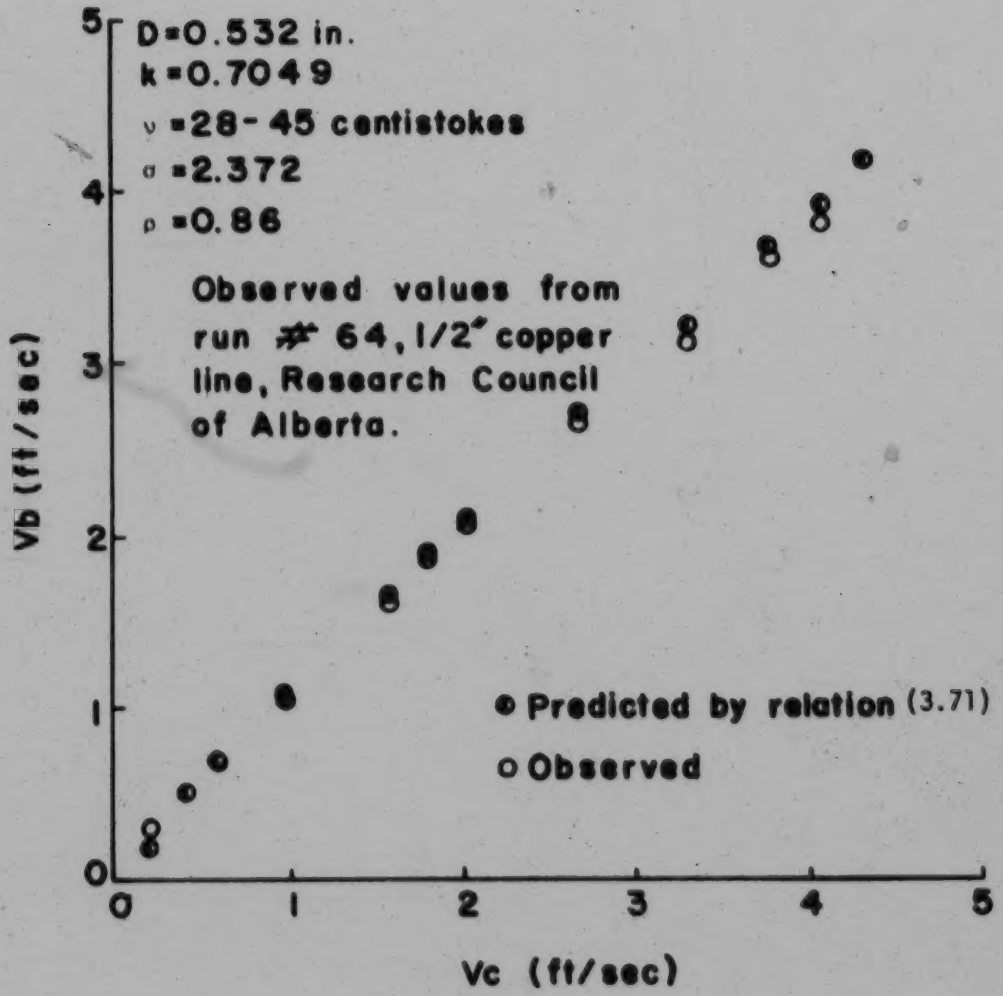

Figure 3.8 Vb versus Vc plots for 1/2" copper line carrying steel capsules in oil.

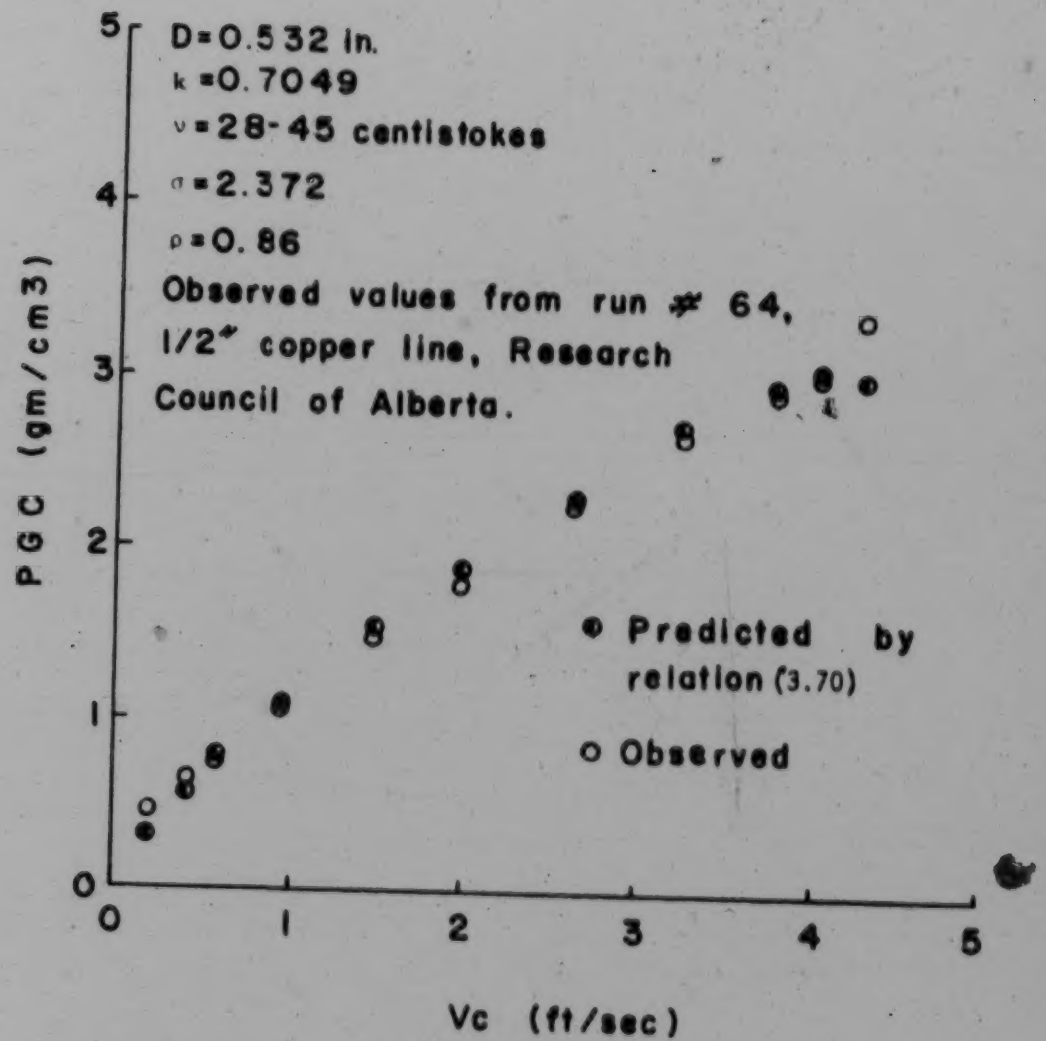

Figure 3.9 PGC versus Vc plots for 1/2" copper line carrying steel capsules in oil.

These conclusions are at best preliminary and need further work. Some independent method of either directly measuring the surface roughness or of inferring these properties would be particularly helpful. Measurements of the actual bottom clearance and angle can be very useful in establishing the capsule flow mechanism and the extent of the secondary flows.

In conclusion then, the slipper-bearing model holds promise as a framework for further analysis. Qualitatively, it explains empirical observations of small bottom clearance, the slight angle with nose-up position for the moving capsule, the effect of surface roughness, the effect of collars, and relationship among the key variables V_b, V_c, and PGC. Further modifications and development may also provide reasonable quantitative agreement with the observed data.

4. CONCLUSIONS

4.1 Summary

The concept of transporting solids in the form of capsules in pipelines evolved at the Research Council of Alberta during the 1950's. Since then, substantial amount of research effort has been devoted in this area with a view to gaining sufficient understanding of the system for possible commercial exploitation. While extensive experimental data have been generated at the Research Council of Alberta and elsewhere, no comprehensive design solution is yet available.

An attempt has been made in Chapter 2 to statistically analyse most of the data available from the Research Council of Alberta to obtain general correlations between the capsule velocity and pressure gradient on the one hand and the independent variables - bulk velocity, liquid viscosity and density, capsule diameter, length and density, and the pipe diameter on the other hand.

While a completely general capacity correlation requires further experimental and modeling work, useful correlations have been obtained for individual pipelines ranging in size from one half of an inch to ten inches. The effect of capsule/pipe diameter ratio, liquid viscosity, capsule/liquid density ratio and the liquid bulk velocity could be modelled. However, the effect of the surfaces' roughness and pipe diameter could not be separately identified due to lack of relevant data.

Little success has been obtained in predicting the pressure drop. The pressure drop data not only had large variance but worse, they were found to be generally not reproducible. This indicates the

presence of variables that have not been taken into account in planning the experiments. It is concluded that the capsule/pipe surface conditions are among the important variables that were not measured.

The second approach to the problem was mechanistic modeling of the capsule flow. A preliminary physical model envisaging the capsule flow as consisting of a series of infinitesimal parallel slipper bearing is presented in Chapter 3. Using a set of simplifying assumptions including one which neglects secondary flows, capacity and pressure drop correlations have been developed for laminar flow. As expected from the assumptions made, the model predictions for both the bulk velocity and the pressure gradient for a given capsule velocity are lower than the observed values. However, addition of only one empirical parameter in the correlations gives reasonable agreement with the observed values. The approach appears to be quite promising.

4.2 Further Work

Considerable amount of further research is required both on experimental and modeling fronts before a complete understanding of the basic fluid mechanics of capsule pipeline flow is possible. Additional controlled data, particularly for pressure drop and empirical modeling of data on the lines described in Chapter 2 are needed. It will also be useful to incorporate secondary flows in the theoretical slipper bearing model developed in Chapter 3.

To obtain a general capacity correlation applicable to a range of pipeline sizes and capsule/pipe surfaces, data should include measurements of coefficient of friction. In addition, a study of changes in capsule/pipe surface roughness over time would be useful

for commercial start up. In experimental runs, the capsule may be run to and fro for a sufficiently long time to achieve ultimate roughness (as defined in section 3.3.1) before pressure drop, velocity and friction data are recorded. To determine the viscosity dependence in the capacity correlation more precisely, data in the viscosity range of 1 c.s. to 20 c.s. for a 1/2" line or 1 c.s. to 30 c.s. in a 1 1/4" line and viscosity varying in a single run from 1 c.s. to 10 c.s. in a 1 1/4" line or from 2 c.s. to 30 c.s. in a 4" line would be helpful.

The model developed in Chapter 3 seems to be a step in the right direction. It is expected that substantial improvements in predictions would result if secondary flows can be incorporated in the model. The secondary flows have the effect of reducing the bottom clearance in the parallel slipper bearing and thus give a higher actual pressure drop than that predicted by the no-leakage bearing model. The treatment for incorporating side leakages (analogous to the secondary flows in the capsule system) is given by Michell (27) and could be used as a starting point.

A more ambitious development of the slipper bearing model would be to divide the annulus into two zones with the liquid in the lower section (of smaller clearance) in laminar flow and in turbulent flow in the upper section. A suitable velocity profile may be assumed for the turbulent flow. The angle including the lower laminar section could be arbitrarily assumed to be a function of Reynolds number.

While we are still a long way from the level of sophistication achieved in the fluid flow, substantial progress has been made as a result of the work done at the Research Council of Alberta. It is felt that further developments in the above direction would significantly improve our understanding of the capsule pipeline flow.

NOTATION

a	distance between the capsule nose and where the line of capsule surface intersects the pipe surface, cm
a_i	dimensionless constants (i = 1, 2, 3, 4, 5)
b_i	empirical parameters (i = 1, 2, 3)
d	capsule diameter, cm
f	drag per unit width of the guide, dyne/cm
g	gravity, cm/sec^2
h	liquid film thickness, cm
k	diameter ratio d/D, dimensionless
p	liquid pressure, dyne/cm^2
p_o	ambient pressure dyne/cm^2
p'	pressure gradient for the capsule system, dyne/cm^3
r	capsule radius, cm
r_1	distance of capsule surface from the center, cm
r_2	distance of the pipe inside surface from the center, cm
u	local liquid velocity, cm/sec
w	vertical force per unit width of the slipper, dyne/cm
x	distance in axial direction, cm
x_i	dimensionless constants (i = 1, ... 9)
y	distance in vertical direction, cm
C_i	integration constants or empirical parameters (i = 1, 2, 3, 4)
D	pipe diameter, cm
E	roughness factor, dimensionless

F	total drag on the capsule, dynes
K_i	functions of k, σ and ρ ($i = 1, \ldots 6$) defined in section 2.4
PGC	pressure gradient for the capsule system, dyne/cm^3 or psi
PGF	pressure gradient when liquid alone flows at the rate of V_b, dyne/cm^3 or psi
PR	pressure ratio PGC/PGF, dimensionless
Q	liquid flow rate per unit of width, cm^2/sec
R	pipe internal radius, cm
S_i	function of σ and ρ ($i = 1, 2$), defined in section 2.4
T	torque on the capsule, dyne-cm
V	velocity, cm/sec or ft/sec
VR	velocity ratio, dimensionless
W	total vertical force, dyne
δ	angle between the infinitesimal capsule surface and the pipe surface, radian
ϵ	eccentricity of the capsule and pipe centres, cm
ℓ	capsule length, cm
ρ	liquid density, g/cm^3
σ	capsule density, g/cm^3
μ	liquid viscosity, poise
ν	liquid kinematic viscosity, stoke or centistoke
θ	angle that the infinitesimal surface makes with the y-direction, radian
τ	shear stress or drag force per unit area, dyne/cm^2
ψ	distance of a liquid shell from centre point, a general functional form

ϕ a general functional form

η coefficient of friction between capsule and pipe surface, dimensionless

Subscripts

an annulus

b bulk

c capsule

ℓ the tail end

m the mid point

o the nose end

p pipe

s stationary

t threshold

x at a distance x from the nose end

C capsule, Couette flow

H horizontal, in the axial direction

P pressure flow

V vertical

BIBLIOGRAPHY

1. Ellis, H. S., Redberger, P. J. and Bolt, L. H., "Transporting Solids by Pipeline Slurries", I. & E.C., 55, No. 8, 19-28 (1963).

2. Charles, M. E., Govier, G. W. and Hodgson, G. W., "Horizontal Pipeline Flow of Equal Density Oil-Water Mixtures", C.J.Ch.E., 39, 27-36 (1961).

3. Charles, M. E. and Hodgson, G. W., "The Pipeline Flow of Capsules, Part 1: The Concept of Capsule Pipelining", C.J.Ch.E., 41, 43-45 (1963).

4. Ellis, H. S., "The Pipeline Flow of Capsules, Part 3: An Experimental Investigation of the Transport by Water of Single Cylinderical and Spherical Capsules with Density Equal to that of Water", C.J.Ch.E., 42, 2, 1-8 (1964).

5. Ellis, H. S., "The Pipeline Flow of Capsules, Part 4: An Experimental Investigation of the Transport in Water of Single Cylinderical Capsules with Density Greater than that of Water", C.J.Ch.E., 42, 2, 69-76 (1964).

6. Ellis, H. S. and Bolt, L. H., "The Pipeline Flow of Capsules, Part 7: An Experimental Investigation of the Transport by Two Oils of Single Cylinderical and Spherical Capsules with Density Equal to that of Oil", C.J.Ch.E., 42, 10, 201-210 (1964).

7. Round, G. F. and Bolt, L. H., "The Pipeline Flow of Capsules, Part 8: An Experimental Investigation of the Transport in Oil of Single, Denser-than-oil, Spherical and Cylinderical Capsules", C.J.Ch.E., 43, 8, 197-205 (1965).

8. Ellis, H. S. and Kruyer, J., "The Pipeline Flow of Capsules, Part 10: Empirical Pressure and Velocity Correlations for Cylinderical Capsules Conveyed in Pipelines up to 4 Inches in Diameter", Hydrotransport 1, First International Conference on the Hydraulic Transport of Solids in Pipes, Paper C2, Warwick, 1st-4th, September 1970.

9. Lazarus, J. H. and Kilner, F. A., "Incipient Motion of Solid Capsules in Pipelines", Hydrotransport 1, First International Conference on the Hydraulic Transport of Solids in Pipes, Paper C3, Warwick, 1st-4th, September 1970.

10. Ellis, H. S., and Kruyer, J., "Some Effects of Fitting Cylinderical Pipeline Capsules with Collars or Runners", Research Council of Alberta Contribution No. 565 (1972).

11. Jensen, E. J. and Berkowitz, N., "The Pipeline Movement of Solids as Capsules and Paste Slugs", Research Council of Alberta Contribution No. 274.

12. Charles, M. E., "The Pipeline Flow of Capsules, Part 2: Theoretical Analysis of the Concentric Flow of Cylinderical Forms", C.J.Ch.E., 41, 4, 46-51 (1963).

13. Kennedy, R. J., "Towards an Analysis of Plug Flow through Pipes", C.J.Ch.E., 44, 10, 354-356 (1966).

14. Kruyer, J., Redberger, P. J. and Ellis, H. S., "The Pipeline Flow of Capsules, Part 9", J. Fluid Mech., 30, 3, 513-531 (1967).

15. Garg, V. K. and Round, G. F., "Capsule Pipeline Flow - A Theoretical Study", paper No. 31, Thermodynamics and Fluid Mech. Convention, University of Glasgow, 1971.

16. Kruyer, J., and Garg, V. K., "Pressure and Couette Flow in a Capsule Pipeline System - Theory and Experiment", Research Council of Alberta, February, 1972.

17. Jensen, E. J., Ellis, H.S., Kruyer, J., White, L. M., Roehl, A. A., "TDA/RCA Capsule Pipeline Project", Information Series No. 63 of Alberta Research, reports I, II and III (1974).

18. Box, G. E. P., Biometrics, 10, 16 (1954).

19. Box, G. E. P. and Hunter, J. S., Technometrics, 4, 301 (1962).

20. Davies, O. L., The Design and Analysis of Industrial Experiments, Oliver and Boyd (1956).

21. Singh, H., "Bayesian Methods in Model Discrimination and Model Building", M.Sc. Thesis, Department of Chemical and Petroleum Engineering, The University of Alberta, Edmonton, Alberta (1971).

22. Quon, D. and Singh, H., "Bayesian Methods in Model Discrimination", to be submitted for publication.

23. Marquardt, D. W., J. Soc. Ind. Appl. Math., 11, 431.

24. Singh, H., Chuang, T., Dalla Lana, I. G. and Quon, D., "Statistical Modeling of the Catalytic Dehydration of 2-Propanol", to be submitted for publication.

25. Prandtl, L., Fluid Dynamics, pp. 153-180, Blackie and Son Ltd., London (1952).

26. Tiedt, W., Technical Report No. 4, Inst. for Hydraulics and Hydrology, Tech. Univ. of Darmstadt (1968), p. 69.

27. Mitchell, A. G. M., Zeitschr, f. Math. u. Phys., Vol. 52, p. 123 (1905).

APPENDIX A

$$F = 2\mu V_c \ell \int_0^{\pi} \left[\frac{3}{R-r-\epsilon_m \cos\theta} - \frac{2}{(R-r-\epsilon_o \cos\theta)}\right] r \, d\theta$$

$$= \frac{2\mu V_c \ell r}{(R-r)} \int_0^{\pi} \left[\frac{3}{\left[1 - \frac{\epsilon_m}{(R-r)} \cos\theta\right]} - \frac{2}{\left[1 - \frac{\epsilon_o}{(R-r)} \cos\theta\right]}\right] d\theta \qquad \text{(A-1)}$$

But

$$\int_0^{\pi} \frac{d\theta}{\left(1 - \frac{\epsilon}{(R-r)} \cos\theta\right)} = \frac{2}{\left[1 - \frac{\epsilon^2}{(R-r)^2}\right]} \arctan \frac{\left(1 + \frac{\epsilon}{R-r}\right) \tan \frac{\theta}{2}}{\left[1 - \frac{\epsilon^2}{(R-r)^2}\right]^{1/2}} \Bigg|_0^{\pi}$$

$$= \frac{\pi}{\left[1 - \frac{\epsilon^2}{(R-r)^2}\right]^{1/2}} \qquad \text{(A-2)}$$

Substituting (A-2) in (A-1)

$$F = \frac{2\pi\mu V_c \ell r}{(R-r)} \left[\frac{3}{\left[1 - \frac{\epsilon_m^2}{(R-r)^2}\right]^{1/2}} - \frac{2}{\left[1 - \frac{\epsilon_o^2}{(R-r)^2}\right]}\right] \qquad \text{(A-3)}$$

APPENDIX B

$$W = 2\int_0^{\pi} w\cos\theta\,(r)\,d\theta$$

$$= 6\ell^2\mu V_c r \int_0^{\pi} \frac{\cos\theta\, d\theta}{(R-r-\epsilon_m\cos\theta)(R-r-\epsilon_\ell\cos\theta)}$$

$$= 6\ell^2\mu V_c r \int_0^{\pi} \left[-\frac{d\theta}{(R-r-\epsilon_m\cos\theta)} + \frac{(R-r)d\theta}{\epsilon_\ell(R-r-\epsilon_m\cos\theta)(R-r-\epsilon_\ell\cos\theta)}\right] \quad \text{(B-1)}$$

Using the results in (A-2)

$$W = \frac{6\ell^2\mu V_c r}{\epsilon_\ell(R-r)}\left[-\frac{\pi}{\left[1-\frac{\epsilon_m^2}{(R-r)^2}\right]^{1/2}} + \int_0^{\pi}\frac{d\theta}{\left[1-\frac{\epsilon_m}{(R-r)}\cos\theta\right]\left[1-\frac{\epsilon_\ell}{(R-r)}\cos\theta\right]}\right]$$

(B-2)

The expression in (B-2) may further be simplified when the angle δ is small so that ϵ_m and ϵ_ℓ are nearly equal, i.e.

$$\left[1-\frac{\epsilon_m}{(R-r)}\cos\theta\right]\left[1-\frac{\epsilon_\ell}{(R-r)}\cos\theta\right] = \left[1-\frac{\epsilon_m+\epsilon_\ell}{2(R-r)}\cos\theta\right]^2 \quad \text{(B-3)}$$

But

$$\left[1-\frac{(\epsilon_m+\epsilon_\ell)^2}{4(R-r)^2}\right]\int_0^{\pi}\frac{d\theta}{\left[1-\frac{\epsilon_m+\epsilon_\ell}{2(R-r)}\cos\theta\right]} = \int_0^{\pi}\frac{d\theta}{\left[1-\frac{\epsilon_m+\epsilon_\ell}{2(R-r)}\cos\theta\right]}$$

$$-\frac{(\epsilon_m+\epsilon_\ell)\sin\theta}{2(R-r)\left[1-\frac{\epsilon_m+\epsilon_\ell}{R-r}\cos\theta\right]}\Bigg|_0^{\pi} \quad \text{(B-4)}$$

or

$$\left[1 - \frac{(\epsilon_m+\epsilon_\ell)^2}{4(R-r)^2}\right]\int_0^\pi \frac{d\theta}{\left[1 - \frac{\epsilon_m+\epsilon_\ell}{2(R-r)}\cos\theta\right]} = \frac{\pi}{\left[1 - \frac{(\epsilon_m+\epsilon_\ell)^2}{4(R-r)^2}\right]^{1/2}} \qquad \text{(B-5)}$$

Hence

$$\int_0^\pi \frac{d\theta}{\left(1 - \frac{\epsilon_m}{R-r}\cos\theta\right)\left(1 - \frac{\epsilon_\ell}{R-r}\cos\theta\right)} = \int_0^\pi \frac{d\theta}{\left[1 - \frac{\epsilon_m+\epsilon_\ell}{2(R-r)}\cos\theta\right]}$$

$$= \frac{\pi}{\left[1 - \frac{(\epsilon_m+\epsilon_\ell)^2}{4(R-r)^2}\right]^{3/2}} \qquad \text{(B-6)}$$

Substituting in (B-2)

$$W = \frac{6\pi\mu\ell^2 V_c r}{\epsilon_\ell(R-r)}\left[\frac{1}{\left[1 - \frac{(\epsilon_m+\epsilon_\ell)^2}{4(R-r)^2}\right]^{3/2}} - \frac{1}{\left[1 - \frac{\epsilon_m^2}{(R-r)^2}\right]^{1/2}}\right] \qquad \text{(B-7)}$$

APPENDIX C

$$T = \int_0^{2\pi} \frac{6\mu V_c}{(2a-\ell)} \cos\theta \left[\int_0^{\ell} \frac{x^2(\ell-x)r\,dx}{h_x^2} \right] d\theta \qquad \text{(C-1)}$$

Substituting for h_x from (3:5)

$$\int_0^{2\pi} \frac{x^2(\ell-x)\ r}{(a-x)^2 \delta^2}\, dx$$

$$= \frac{r}{\delta^2} \left[-x - (2a-\ell) + \frac{a(3a-2\ell)}{(a-x)} - \frac{(a-\ell)a^2}{(a-x)^2} \right] dx$$

$$= \frac{r}{\delta^2} \left[-\frac{x^2}{2} - (2a-\ell)x - a(3a-2\ell)\ \ell n\ (a-x) - \frac{(a-\ell)a^2}{(a-x)} \right]_0^{\ell}$$

$$= \frac{r}{\delta^2} \left[-\frac{\ell^2}{2} - (2a-\ell)\ell + a(3a-2\ell)\ \ell n\ \left(\frac{a}{a-\ell}\right) - a\ell \right] \qquad \text{(C-2)}$$

When the angle δ is small, i.e. $a \gg \ell$, $\ell n\left(\frac{a}{a-\ell}\right)$ may be approximated by the first two terms of its Taylor series.

$$\ell n\ \left(\frac{a}{a-\ell}\right) = \ell n\left(1 - \frac{\ell}{a-\ell}\right) = \frac{\ell}{(a-\ell)} - \frac{1}{2}\frac{\ell^2}{(a-\ell)^2} \qquad \text{(C-3)}$$

Substituting in (C-2) and simplifying

$$\int_0^{\ell} \frac{x^2(\ell-x)\ r}{(a-x)^2\ \delta^2}\, dx = \frac{r}{\delta^2} \left[-3a\ell + \frac{\ell^2}{2} + \frac{a\ell(3a-2\ell)}{(a-\ell)} - \frac{1}{2}\frac{a\ell^2(3a-2\ell)}{(a-\ell)^2} \right]$$

$$= \frac{r}{\delta^2}\left[\frac{\ell^2(3a-\ell)}{2(a-\ell)} - \frac{a\ell^2(3a-2\ell)}{2(a-\ell)^2}\right]$$

$$= -\frac{r}{\delta^2}\,\frac{\ell^3(2a-\ell)}{2(a-\ell)^2} \qquad \text{(C-4)}$$

Substituting in (C-1)

$$T = -\int_0^{2\pi} \frac{6\mu V_c\, r\, \ell^3 \cos\theta}{2(a-\ell)^2\,\delta^2}$$

$$= -6\mu V_c \ell^3 \int_0^{\pi} \frac{r}{h_\ell^2}\cos\theta\, d\theta$$

$$= -6\mu V_c \ell^3 \int_0^{\pi} \frac{r\cos\theta}{(R-r-\epsilon_\ell\cos\theta)^2}\, d\theta$$

$$= -6\mu V_c \ell^3 r \int_0^{\pi} \left[\frac{(R-r)}{\epsilon_\ell(R-r-\epsilon_\ell\cos\theta)^2} - \frac{1}{\epsilon_\ell(R-r-\epsilon_\ell\cos\theta)}\right] d\theta \qquad \text{(C-5)}$$

Utilizing the results in (A-2) and (B-5)

$$T = \frac{6\pi\mu V_c \ell^3 r}{\epsilon_\ell(R-r)}\left[\frac{1}{\left[1-\frac{\epsilon_\ell^2}{(R-r)^2}\right]^{3/2}} - \frac{1}{\left[1-\frac{\epsilon_\ell^2}{(R-r)^2}\right]^{1/2}}\right]$$

$$= \frac{6\pi\mu V_c \ell^3 r\,\epsilon_\ell}{(R-r)^3\left[1-\frac{\epsilon_\ell^2}{(R-r)^2}\right]^{3/2}} \qquad \text{(C-6)}$$

APPENDIX D

$$Q_p = \int_0^{2\pi} d\theta \int_{r_2}^{r_1} u \, r \, d\psi \qquad \text{(D-1)}$$

$$= 2 \int_0^{\pi} q_p \, d\theta$$

where

$$q_p = \int_{r_2}^{r_1} u \, r \, d\psi \qquad \text{(D-2)}$$

may be considered as flow per unit of angle around O (Figure 3.4).

Substituting for u from (3.36)

$$q_p = \frac{PGC}{4\mu} \int_{r_2}^{r_1} \left[-\psi^3 + \frac{(r_1^2 - r_2^2)}{\ln \frac{r_1}{r_2}} \psi \ln \psi \right.$$

$$\left. + \frac{(r_2^2 \ln r_1 - r_1^2 \ln r_2)}{\ln \frac{r_1}{r_2}} \psi \right] d\psi$$

$$= \frac{PGC}{16\mu} \left[\psi^4 + \frac{(r_1^2 - r_2^2)}{\ln \frac{r_1}{r_2}} (2\psi^2 \ln \psi - \psi^2) \right.$$

$$\left. + \frac{(r_2^2 \ln r_1 - r_2^2 \ln r_2)}{\ln \frac{r_1}{r_2}} (2\psi^2) \right|_{r_1}^{r_2} \qquad \text{(D-3)}$$

Taking the limits and simplifying

$$q_p = \frac{PGC}{16\mu}(r_1^2 - r_2^2)\left[r_1^2 + r_2^2 - \frac{(r_1^2 - r_2^2)}{\ln \frac{r_1}{r_2}}\right] \qquad \text{(D-4)}$$

The natural log may be approximated by the first two terms of its series expansion when $(r_1-r_2)/r_2$ is small, i.e.

$$\ln \frac{r_1}{r_2} = \ln\left[1 + \frac{r_1-r_2}{r_2}\right]$$

$$\frac{r_1-r_2}{r_2} - \frac{1}{2}\frac{(r_1-r_2)^2}{r_2^2}$$

$$= \frac{r_1-r_2}{r_2}\left[1 - \frac{1}{2}\frac{r_1-r_2}{r_2}\right] \qquad \text{(D-5)}$$

or

$$\frac{1}{\ln \frac{r_1}{r_2}} = \frac{r_2}{r_1-r_2}\left[1 - \frac{1}{2}\frac{r_1-r_2}{r_2}\right]^{-1}$$

$$= \frac{r_2}{r_1-r_2}\left[1 + \frac{1}{2}\frac{r_1-r_2}{r_2}\right]$$

$$= \frac{r_2}{r_1-r_2} + \frac{1}{2} \qquad \text{(D-6)}$$

Substituting (D-6) in (D-4) yields

$$q_p = \frac{PGC}{32\mu}(r_1+r_2)(r_1-r_2)^3 \qquad \text{(D-7)}$$

Now

$$r_1 = R - \frac{t}{2}\cos\theta \qquad r_2 = r + \frac{t}{2}\cos\theta$$

$$R - \frac{t_m}{2}\cos\theta \qquad r + \frac{t_m}{2}\cos\theta$$

and

$$t_m = \frac{(R-r)}{2}$$

Thus

$$q_p = \frac{PGC}{32\mu}(R+r)(R-r)^3\,[1 - 3\cos\theta + 3\cos^2\theta - \cos^3\theta] \qquad \text{(D-8)}$$

$$Q_p = \frac{2(PGC)(R^2-r^2)(R-r)^2}{32\mu}\int_0^{\pi}[1 - 3\cos\theta + 3\cos^2\theta - \cos^3\theta]\,d\theta \qquad \text{(D-9)}$$

Noting that

$$\int \cos\theta\,d\theta = \sin\theta$$

$$\int \cos^2\theta\,d\theta = \frac{\sin\theta\cos\theta}{2} + \frac{1}{2}\theta \qquad \text{(D-10)}$$

$$\int \cos^3\theta\,d\theta = \frac{\sin\theta\cos^2\theta}{2} + \frac{2}{3}\sin\theta$$

and that $k = \frac{r}{R}$

(D-9) simplifies to

$$Q_p = \frac{5\pi R^4 (PGC)}{32\mu}(1-k^2)(1-k)^2 \qquad \text{(D-11)}$$

APPENDIX E

Substituting f_c from (3.19) and ϵ_p from (3.44) in (3.46) and using the mean clearance ϵ_m for ϵ.

$$T_h = \int_0^{2\pi} \left[\frac{3\mu V_c \ell}{h_m} - \frac{2\mu V_c \ell}{h_o} \right] r^2 (1 - \cos\theta)\, d\theta$$

$$- \int_0^{2\pi} \frac{(PGC)\, \ell r^2}{4r_2} \left[\frac{1}{2} (r_1 + r_2)^2 - 2r_2^2\right] (1-\cos\theta)\, d\theta$$

$$= 2\mu V_c \ell r^2 \int_0^{\pi} \left[\frac{3(1-\cos\theta)\, d\theta}{(R-r-\epsilon_m\cos\theta)} - \frac{2(1-\cos\theta)\, d\theta}{(R-r-\epsilon_o\cos\theta)}\right]$$

$$- \frac{(PGC)\, \ell\, r^2}{8} \int_0^{\pi} \left[\frac{(R+r)(R-r-\epsilon_m\cos\theta)(1-\cos\theta)}{(r + \frac{\epsilon_m}{2}\cos\theta)} \right.$$

$$\left. + 2(R-r-\epsilon_m \cos\theta)(1-\cos\theta)\, d\theta\right] \qquad \text{(E-1)}$$

Using the result in (A-1)

$$\int_0^{\pi} \frac{(1-\cos\theta)\, d\theta}{(R-r-\epsilon\cos\theta)} = \int_0^{\pi} \left[\frac{1}{\epsilon} - \frac{R-r-\epsilon}{(R-r-\epsilon\cos\theta)}\right] d\theta$$

$$= \frac{\pi}{\epsilon} - \frac{(R-r-\epsilon)\, \pi}{\epsilon(R-r)\left[1 - \frac{\epsilon^2}{(R-r)^2}\right]^{1/2}} \qquad \text{(E-2)}$$

and

$$\int_0^{\pi} \frac{(R-r-\varepsilon_m \cos\theta)(1-\cos\theta)}{(r+\frac{\varepsilon_m}{2}\cos\theta)}$$

$$= \int_0^{\pi} \left[2\cos\theta - \frac{2(\varepsilon_m+R+r)}{\varepsilon_m} + \frac{(R+r)(\varepsilon_m+2r)}{\varepsilon_m(r+\frac{\varepsilon_m}{2}\cos\theta)}\right] d\theta$$

$$= -\frac{2\pi(\varepsilon_m+R+r)}{\varepsilon_m} + \frac{(R+r)(\varepsilon_m+2r)\pi}{\varepsilon_m r\left[1+\frac{\varepsilon_m}{4r^2}\right]^{1/2}} \qquad \text{(E-3)}$$

Also

$$\int_0^{\pi} (R-r-\varepsilon_m \cos\theta)(1-\cos\theta)\, d\theta$$

$$= \int_0^{\pi} [(R-r) - (R-r+\varepsilon_m)\cos\theta + \varepsilon_m \cos^2\theta] d\theta$$

$$= \pi\,(R-r+\frac{\varepsilon_m}{2}) \qquad \text{(E-4)}$$

Substituting (E-2), (E-3) and (E-4) in (E-1) gives

$$T_R = 2\pi\mu V_c \ell r^2 \left(\frac{3}{\varepsilon_m} - \frac{2}{\varepsilon_o} - \frac{3(R-r-\varepsilon_m)}{\varepsilon_m(R-r)\left(1-\frac{\varepsilon_m^2}{(R-r)^2}\right)^{1/2}} + \frac{2(R-r-\varepsilon_o)}{\varepsilon_o(R-r)\left(1-\frac{\varepsilon_o^2}{(R-r)^2}\right)^{1/2}}\right)$$

$$+ \frac{\pi(PGC)\,\ell\, r^2}{8}\left(\frac{2(\varepsilon_m+R+r)(R+r)}{\varepsilon_m} - \frac{(R+r)^2(\varepsilon_m+2r)}{\varepsilon_m r\left(1+\frac{\varepsilon_m}{4r^2}\right)^{1/2}} + 2(R-r-\frac{\varepsilon_m}{2})\right) \qquad \text{(E-5)}$$

APPENDIX F

When the clearance and the angle δ are small so that $\epsilon_m \approx \epsilon_\ell + \epsilon_o = (R-r)$, we may replace ϵ_ℓ and ϵ_o by ϵ_m and ϵ_m by $(R-r)$ where the expression is not very sensitive to ϵ_m.

Thus (3.52) reduces to

$$\left[1 - \frac{\epsilon_m^2}{(R-r)^2}\right] = \left[\frac{6\mu\ell V_c}{\epsilon_m r(\sigma-\rho)\, g(R-r)}\right]^{2/3} \qquad \text{(F-1)}$$

For example, the R.H.S. is not sensitive to the value of ϵ_m and may be replaced by $(R-r)$ as an approximation but the L.H.S. is very sensitive to the value of ϵ_m ($\epsilon_m = R-r$ would reduce it to zero). The effect of such approximation depends upon the value of ϵ_m, ϵ_o and ϵ_ℓ. As an example, a bottom mean clearance of $[h_m/(R-r)] = 0.0001$ and $h_\ell = \frac{h_m}{2}$ would introduce an error of around one—hundredth of one percent in approximating relation (3.52) to (F-1).

Thus

$$1 - \frac{\epsilon_m^2}{(R-r)^2} = \left[\frac{6\mu\ell V_c}{(R-r)^2 r(\sigma-\rho)\, g}\right]^{2/3} \qquad \text{(F-2)}$$

or

$$\epsilon_m = (R-r)\sqrt{1 - \left[\frac{6\mu\ell V_c}{(R-r)^2 r(\sigma-\rho)\, g}\right]^{2/3}} \qquad \text{(F-3)}$$

Similarly (3.53) reduces to

$$PGC = \frac{16\mu V_c k}{R^2(1-k)(1+6k+k^2)} \left(\frac{1}{\left(1 - \frac{\epsilon_m^2}{R^2(1-k)^2}\right)^{1/2}}\right) \qquad \text{(F-4)}$$

Substituting (F-2) in (F-3)

$$PGC = \frac{8\mu k V_c^{2/3}}{R(1+6k+k^2)} \left[\frac{4k(\sigma-\rho)g}{3(1-k)\mu\ell}\right]^{1/3} \tag{F-5}$$

Substituting in (3.49)

$$V_b = \frac{5k(1-k)^2(1-k^2)}{4(1+6k+k^2)} \left[\frac{4k(\sigma-\rho)\,g}{3(1-k)\mu\ell}\right]^{1/3} R\, V_c^{2/3} + \frac{1}{2}(1+k^2)\, V_c \tag{F-6}$$

For high viscosity liquids, the first term is probably quite small so that

$$V_c = \frac{2}{(1+k^2)} V_b \tag{F-7}$$

Substituting in (F-5)

$$PGC = \frac{16\mu V_b k}{R(1+k^2)(1+6k+k^2)} \left[\frac{2k(1+k^2)(\sigma-\rho)\, g}{3(1-k)\,\mu\ell V_b}\right]^{1/3} \tag{F-8}$$

APPENDIX C

```
⍝  THE PROGRAM 'PLOT' PLOTS ON Z×Y SCALE THE COLUMNS
⍝  OF 'X' MATRIX AGAINST THE FIRST COLUMN BY THE
⍝  COMMAND Z Y PLOT X.


)PLOT[□]⍝
     ∇ A PLOT B;C;D;F;G;H;I;J;L;T;Y;HZ;HP;VT;PT;ST;ISV;P
       ;SZ;SW
[1]    PC←'O*•∇A□'
[2]    HZ←0
[3]    SZ← 1 2 5
[4]    SW← 5 10
[5]    →((0=×/(2⍴A),⍴B),3 2 1 <⍴⍴B)/0,PL7,PL1,PL2
[6]    →PL2,⍴B←B(2,D)⍴(1↑D←⍴,B),B
[7]   PL1:B←B[1;;]
[8]   PL2:Y←1+1↓(⍴B)[2]-1
[9]    C←((⌈/⌈/B[;Y])-1⌊1⌊/B[;Y]),(⌈/B[;1])-1⌊/B[;1]
[10]   D←|(2⍴A)↑C+(C=0)×B[1; 2 1]+B[1; 2 1]=0
[11]   F←(SZ[+/(|0.0001+F×10*-G)•.≥SZ])×10*G←|10⊥D
[12]   G←(SW↑F)×|((1⌊1⌊/B[;Y]),1⌊/B[;1])×F↑SW←16|SW[ 1
       4
[13]   B[;1]←|0.5+B[2]×B[;1]-C[2]
[14]   B[;Y]←|0.5+B[1]×B[;Y]-C[1]
[15]   B←SW×⌈(((⌈/⌈/B[;Y]),⌈/B[;1])↑SW
[16]   HP←C[1]+(SW[1]↑B[1])×0,1↓B[1]↑SW[1]
[17]   HZ←C[2]+(SW[2]↑B[2])×0,1↓B[2]↑SW[2]
[18]   0⍴ST←60⍴~ISV←1×U←9
[19]  PL3:VT←∨/0>HP←HP×10*U-ST[6-ISV]←T←1+⌈/|10⊥|(HP×0)/HP
[20]   PT←|1+10|PT-1|PT←1⊥¯5+(|HP)•.↑10*¯1+⍳U
[21]   L←U+1-(⍳((C←⍴HP)⍴1)∧.=PT)⍳0
[22]   →((U≥T←VT+⌈/T,(L+L×T),(T≤0)×2+L-T),ST[2-ISV]←ST[
       2-ISV]∨L≥U-VT+L>T)/ 3 2 +I26
[23]   →(¯1+I26),⍴ST[4-ISV]←T←1
[24]   →PL3,⍴HP←SW[1+~ISV]×¯1+C
[25]   PT←(-VT+0⌈1-T)⌽PT
[26]   PT←(,PT)×J←,⍉(⌽⍴PT)⍴(,⍉(1×PT)∨.∧(⍳U)•.≤⍳VT[T-1]),(C×U+1-
       T←VT+T[T≤0])⍴1
[27]   →(~VT)/2+I26
[28]   PT[(U-+/(C,U)⍴J)+U×¯1+⍳C]←11×HP<0
[29]   PT←(~(⍳U+J)∈(T+J),⍳¯1+J←U-T)\(1 0 +C,U)⍴PT,U⍴0
[30]   PT[⍳C;T+J]←12
[31]   PT←' 0123456789¯.'[1+PT[;⍳U-1]]
[32]   →(~ISV)/PL6
[33]   L←1,B[2]⍴0×C←B[1]
[34]  PL4:L←(L×PS×C×0)⌈1,B[2]⍴0
[35]   L[1+(D×0)/B[;1]]←(D×0)/D←(C=B[;Y])⌈.×Y
[36]   →(C×0)/PL5
[37]   L←L[0=(SW[2]↑2)|0,⍳B[2]
[38]  PL5:PT[((⍴PT)[1],1+C↑SW[1])[1+0=SW[1]|C];],(' |',(⍴Y)⍴PC
       )[1+L]
```

```
⍝   PROGRAM 'PLOT' CONTINUED ....


∇PLOT[□39] ∇
[39]   →(0≤C←C-1)/PL4
[40]   →(U=U←SM[2]-~⍴SV←~⍴0⍴HP←,PT)/PL3
[41] PL6:(SM[2]-9)⍴(,(0 0 ,(U-1)⍴1)\PT),' '
[42]   →(ST[1 3 2 4],1)/ 1 3 5 7 10 ⍴I26
[43]   'ORIGIN AND SCALE FACTOR FOR ORDINATE: ';G[1],⍴F[1]
[44]   →(0=ST[3])/2⍴I26
[45]   'SCALE FACTOR FOR ORDINATE: ';10*ST[5]-1
[46]   →(0=ST[2])/2⍴I26
[47]   'ORIGIN AND SCALE FACTOR FOR ABSCISSA: ';G[2],⍴F[
       2]
[48]   →(0=ST[4])/0
[49]   'SCALE FACTOR FOR ABSCISSA: ';10*ST[6]-1
[50]   →0
[51] PL7:'THE RIGHT ARGUMENT OF  PLOT  MUST HAVE RANK ≤ 3.'
[51]   ∇


⍝   THE PROGRAM 'LINN' ESTIMATES THE LEAST SQUARE PARAMETERS
⍝    , VARIANCE OF FIT, RESIDUAL ERRORS AND CONFIDENCE LIMITS
⍝   OF PARAMETERS FOR A LINEAR MODEL.


∇LINN[□]∇
    ∇ LINN;N;M;A;C95;I;C;SS;ER;D
[1]    N←⍴Y
[2]    M←⍴X[1;]
[3]    A←⌹(⍉X)+.×X
[4]    B←A+.×(⍉X)+.×Y
[5]    ER←Y-X+.×B
[6]    SS←+/ER*2
[7]    VAR←SS÷(N-M)
[8]    C←VAR×A
[9]    'PARAMETERS :      ';B
[10]   D←(⍴,M)⍴0
[11]   C95←M⍴0
[12]   I←0
[13] LAB:I←I+1
[14]   C95[I]←2×C[I;I]*0.5
[15]   D[I;I]←C[I;I]*¯0.5
[16]   →LAB×ι I<M
[17]   C←D+.×C+.×D
[18]   '95 PCNT LIMITS : ';C95
[19]   'VAR : ';VAR;' STD DEV : ';VAR*0.5
[20]   'CORR MAT : ';C
[21]   'NORMAL ERRORS : ';ER÷VAR*0.5
[22] ERR:→ι0
    ∇
```

```
⍝   THE PROGRAM 'NLGT' ESTIMATES THE LEAST SQUARE PARAMETERS
⍝   ,VARIANCE OF FIT, RESIDUAL ERRORS AND CONFIDENCE LIMITS
⍝   OF PARAMETERS FOR A NON-LINEAR MODEL. IT FOLLOWS THE
⍝   ITERATIVE ALGORITHM DEVELOPED BY MARQUARDT(REF. 23).


∇NLGT[⎕]∇
    ∇ NLGT;S1;S2;D1;D2;G;I;IL;IT;R1;R2;RR;C95;PH1;PH2;P;PP;
[1]   LA←1
[2]   Y←⍞
[3]   P←⍞
[4]   IT←0
[5]   Y←(,Y)∘.=1
[6]   LRR:PH1←P PUCH L
[7]   X←P DSH L
[8]   G←(⍉X)+.×(Y-PH1)
[9]   SS←(⍉(Y-PH1))+.×(Y-PH1)
[10]  A←((⍉X)+.×X)
[11]  D1←D2←I
[12]  IL←0
[13] LAS:IL←IL+1
[14]  D1[IL;IL]←(A[IL;IL]+LA)*¯0.5
[15]  D2[IL;IL]←(A[IL;IL]+LA×NU)*¯0.5
[16]  →LAS×⍳IL<N
[17]  D1←(D1+.×(⍉D1+.×(A+LA×T)+.×D1)+.×D1)+.×G
[18]  D2←(D2+.×(⍉D2+.×(A+(LA×NU)×T)+.×D2)+.×D2)+.×G
[19]  D1←P+D1
[20]  D2←P+D2
[21]  PP←P
[22]  P←D1
[23]  PH1←P PUCH L
[24]  P←D2
[25]  PH2←P PUCH L
[26]  S1←(⍉(Y-PH1))+.×(Y-PH1)
[27]  S2←(⍉(Y-PH2))+.×(Y-PH2)
[28]  →THRE×⍳((|((+/((PP-D1)÷PP)))<0.0001)
[29]  →OVF×⍳S2≤SS
[30]  →TWO×⍳S1>SS
[31] P←D1
[32]  SS←S1
[33]  →LRC
[34] OVF:LA←LA×NU
[35]  →OVF1×⍳S2≤S1
[36]  P←D1
[37]  SS←S1
[38]  →LRC
[39] OVF1:P←D2
[40]  SS←S2
[41]  →LRC
[42] TWO:LA←LA×NU
[43]  P←PP
[44] LRC:P,SS
[45]  →LRR
[46] THRE:→FOUR×⍳SS<S1
[47]  X←P DSH L
```

```
⍝   PROGRAM 'UGT' CONTINUED....


∇UGT[[]47]
[47]  X←P PSP" L"
[48]  SS←S1
[49]  PP←Y-PRT1
[50]  →PRINT
[51]  POWP:P←PP
[52]  PP←Y-PRT
[53]  PRINT:'PARAMETERS : ';P
[54]  VAR←SS÷N-"
[55]  C←VAR×(⍉(⊗X)+.×X)
[56]  C95←P
[57]  P←I
[58]  I←0
[59]  LST:I←I+1
[60]  C95[I]←2×(C[I;I]*0.5)
[61]  P[I;I]←C[I;I]*-0.5
[62]  →LST×⍳I<N"
[63]  '95 PCNT LMT: ';C95
[64]  'VARIANCE : ';VAR;'STD DEV : ';STD←VAR*0.5
[65]  'COEF MAT :';P+.×C+.×P
[66]  'NORMAL ERRORS:';PP÷STD
[67]  'MODEL LINEARIZED: ';L←VAR PST SS
[67]  ∇


⍝   THE PROGRAM 'FUGU' STORES THE MODEL FUNCTIONAL
⍝   FORM FOR USE IN 'UGT'.


∇FUGU[[]]∇
    ∇ PRT←P FUGU L"
[1]   →FOUR×⍳L"=4
2]  [→THRE×⍳L"=3
3]    →TWO×⍳L"=2
4]    →SIX×⍳L"=6
5]    →SEVEN×⍳L"=7
[6]   ONE:PRT←P[1]×((((1-XA)*1.5)*NF)*2×P[2])×(((XS-1)*XS))
[7]   →PRINT
[8]   TWO:PRT←P[1]+P[2]×VAV*P[3]
[9]   →PRINT
[10]  THRE:PRT←P[1]×((XS-1)*P[2])×(1-XA*2)×(1-XA*4)
[11]  →PRINT
[12]  FOUR:PRT←P[1]×(((XS-1))*P[2]×(1-XA*2))×(1-XA)
[13]  →PRINT
[14]  SIX:PRT←P[1]×T×(*-P[2]*1.987×T)×(1-*-P[3]×Z*P[4])
[15]  PRINT:→10
   ∇
```

```
⍝   THE PROGRAM 'DSHM' STORES THE DERIVATIVES OF THE MODEL
⍝   WITH RESPECT TO THE PARAMETERS FOR USE IN 'MGT'.


∇DSHM[⎕]∇
     ∇ X←R DSHM L;M
[1]    M←⍴R
[2]    X←(⍳M)∘.=⍳M
[3]    →ONE×⍳L=1
[4]    →TWO×⍳L=2
[5]    →THRE×⍳L=3
[6]    →FOUR×⍳L=4
[7]    →SIX×⍳L=6
[8]   ONE:X[;1]←PHI⍟R[1]
[9]    X[;2]←PHI×2×⍟((1-XA)÷1.5)÷HF
[10]   →THE
[11] TWO:X[;1]←1
[12]   X[;2]←VAV÷R[3]
[13]   X[;3]←R[2]×(⍟VAV)×VAV÷R[3]
[14]   →THE
[15] THRE:X[;1]←PHI⍟R[1]
[16]   X[;2]←PHI×(⍟XS-1)
[17]   →THE
[18] FOUR:X[;1]←PHI⍟R[1]
[19]   X[;2]←PHI×(1-XA÷2)×(⍟(XS-1))
[20]   →THE
[21] SIX:X[;1]←PHI⍟R[1]
[22]   X[;2]←-PHI÷1.987×T
[23]   X[;3]←R[1]×T×(Z÷R[4])×(⍟-R[2]÷1.987×T)×(⍟-R[3]×Z÷R[4])
[24]   X[;4]←X[;3]×R[3]×(⍟Z)
[25]   →THE
[26] THE:→0
     ∇
```